CIBM Center for Biomedical Imaging

BASICS OF MR SPECTROSCOPY

Lijing Xin

CIBM EPFL MRI

27.04.2023

CHUV   Unil UNIL | Université de Lausanne   EPFL   UNIVERSITÉ DE GENÈVE   HUG Hôpitaux Universitaires Genève

C I B M . C H

Lijing.xin@epfl.ch

OUTLINE

- Introduction of MRS (chemical shift and J-coupling)
- Localization techniques
- B_0 Shimming
- B_1^+ calibration
- Water suppression
- Outer volume suppression

C I B M . C H

CHEMICAL SHIFT AND J-COUPLING

RESONANCE FREQUENCY

7T
300MHz

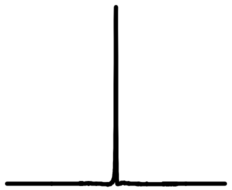

Resonance frequency of a nucleus $\omega_0 = \gamma B_0$

The Dependence of a Nuclear Magnetic Resonance Frequency upon Chemical Compound*

W. G. Proctor and F. C. Yu

Department of Physics, Stanford University, Stanford, California

January 18, 1950

Glutamate

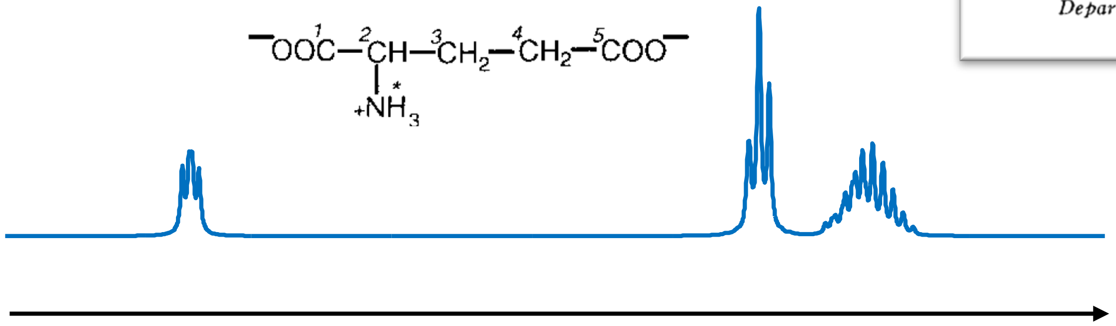

f

nuclei in a molecule resonant at different frequencies

SHIELDING AND RESONANCE FREQUENCY

Lenz's law

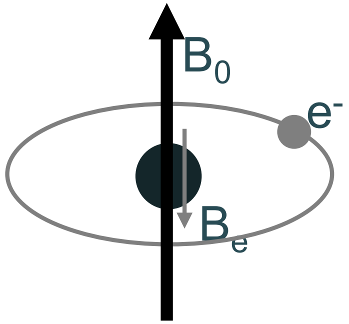

$$B_{eff} = B_0 - B_e = B_0(1 - \sigma)$$

σ , the shielding constant

Lactate

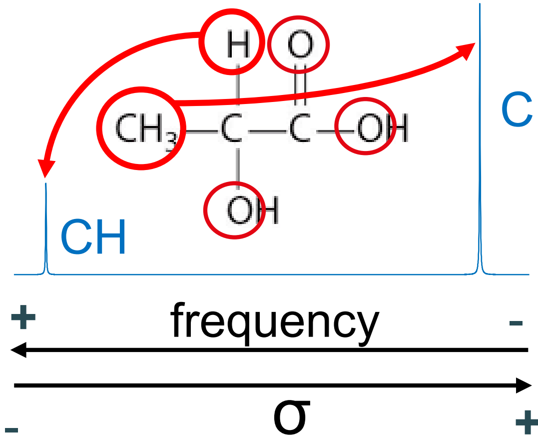

low electron density

high electron density

Electronegativity

C	N	O
2.55	3.04	3.44

$$\omega_0 = \gamma B_0(1 - \sigma)$$

Electrons around the nucleus shield it from the applied field

Resonance frequency depends on the chemical environment of the nucleus

CHEMICAL SHIFT

Chemical shift in *parts per million*
(magnetic field independent)

$$\delta = \frac{\omega - \omega_{ref}}{\omega_{ref}} \times 10^6$$

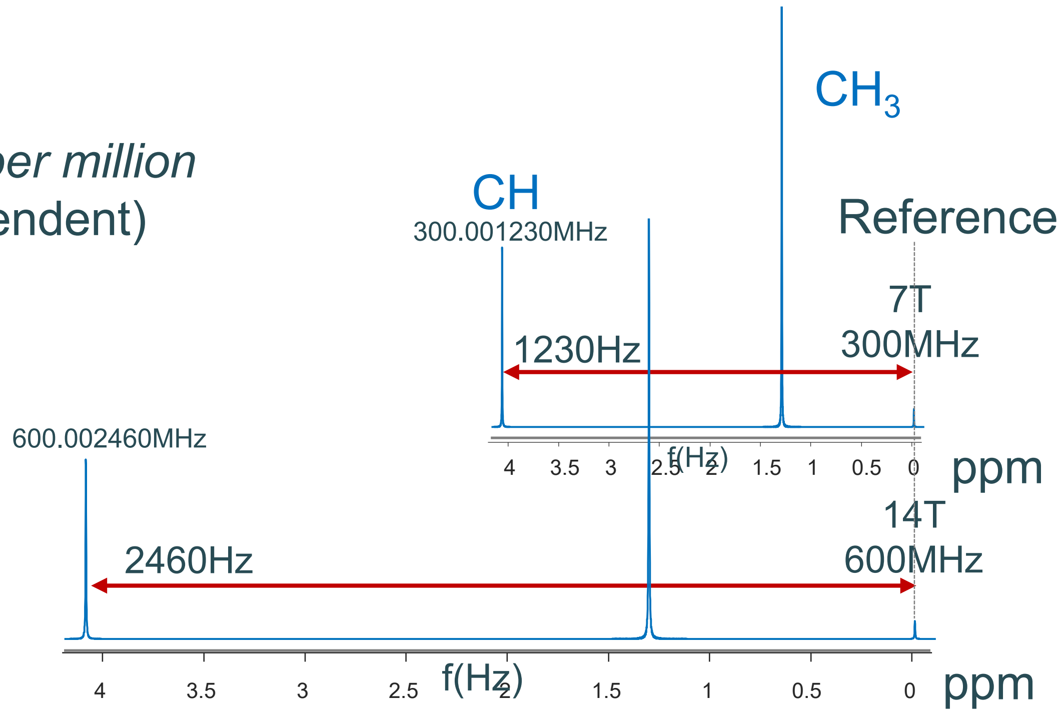

J-COUPLING

J-coupling (spin-spin coupling, scalar coupling)

Interactions between neighboring nuclear spins

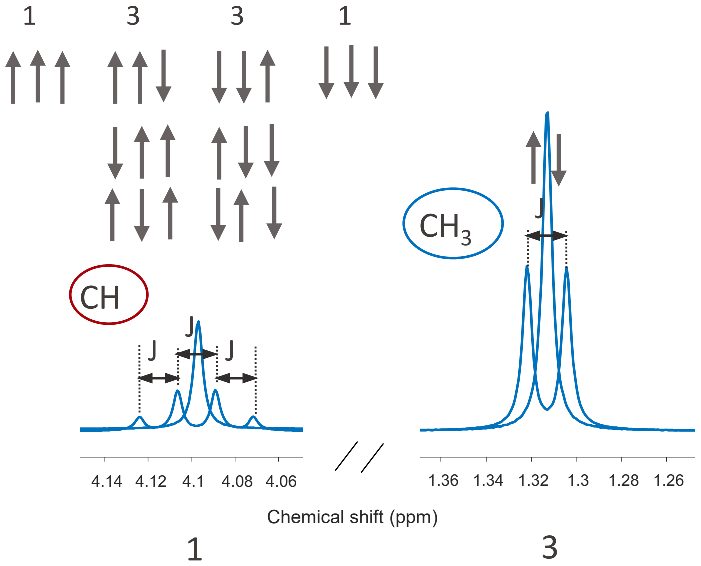

Integral of resonances ∝ number of nuclei

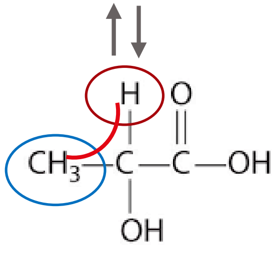

Lactate

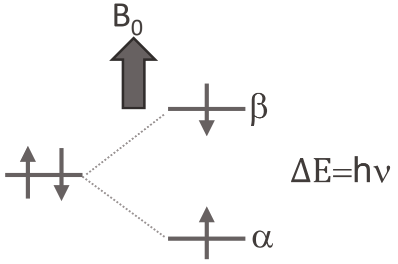

Number of splitting peaks: n+1

n: the number of neighboring identical nuclei

J: coupling constant in Hz

n	Pascal's triangle
0	1
1	1 1
2	1 2 1
3	1 3 3 1
4	1 4 6 4 1
5	1 5 10 10 5 1
6	1 6 15 20 15 6 1
7	1 7 21 35 35 21 7 1
8	1 8 28 56 70 56 28 8 1

MORE ABOUT J-COUPLING

- J is independent of the magnetic field

- Peak splitting
  - Weakly coupled ($|v_1 - v_2| \gg J_{12}$), e.g. ^1H-^{13}C, product operator formalism
  - Strongly coupled (roof effect): e.g. ^1H-^1H, density matrix formalism

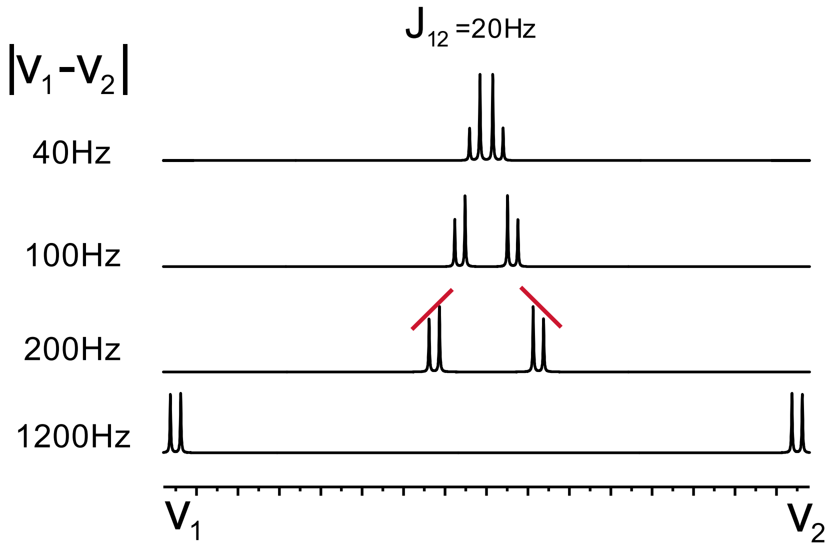

FINGERPRINTS OF MOLECULES

Chemical shift
J-coupling

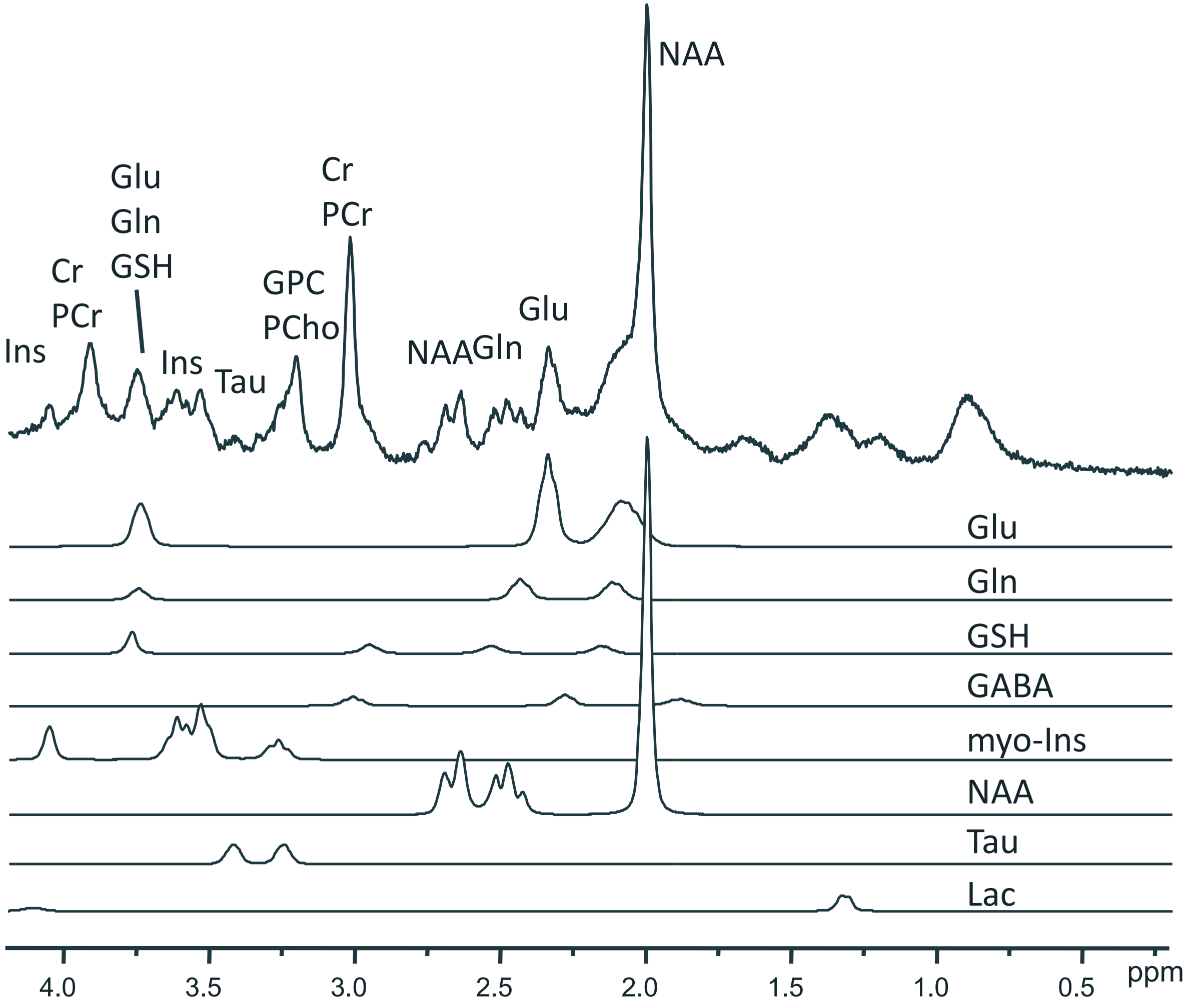

CIBM.CH

J-EVOLUTION WITH TE

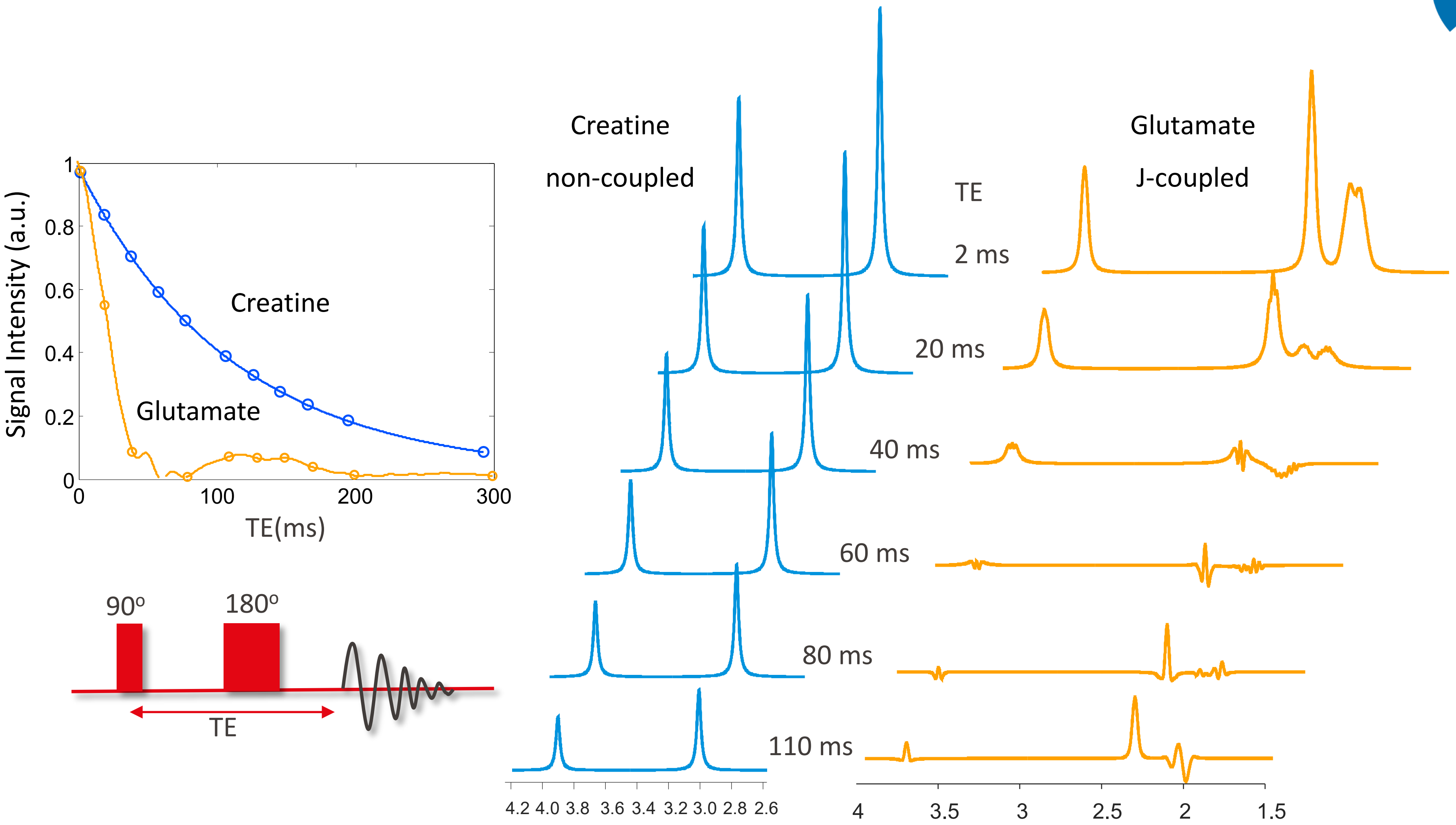

LOCALIZATION METHODS

LOCALIZATION WITH SURFACE COIL

surface coil

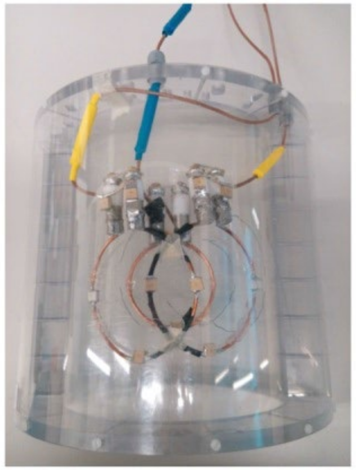

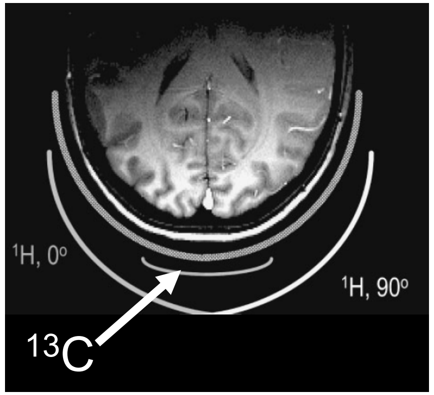

Lipid contamination

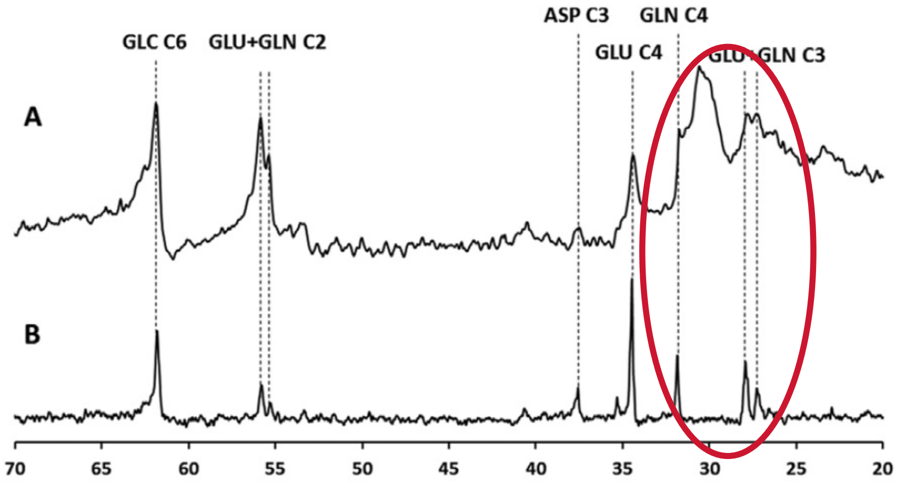

Valette et al., Anal. Biochem., 529,.216-228, 2017

CIBM.CH

PRINCIPLE OF LOCALIZATION

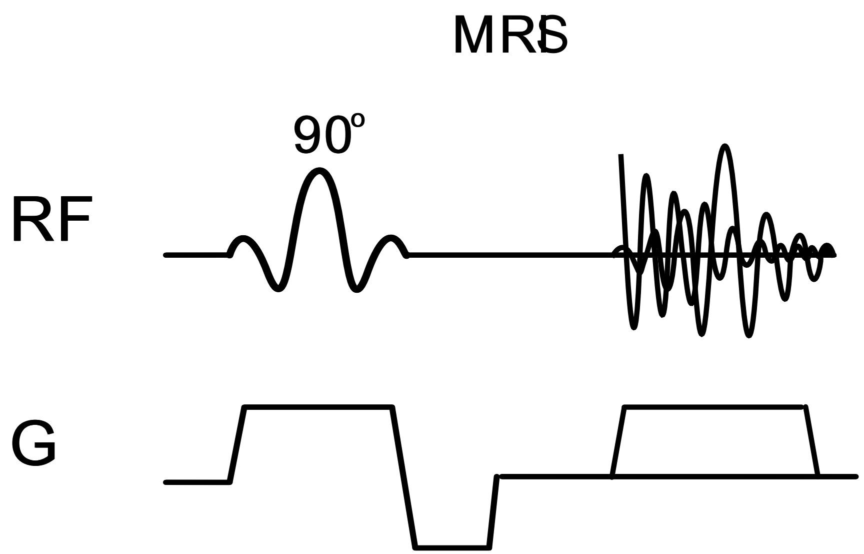

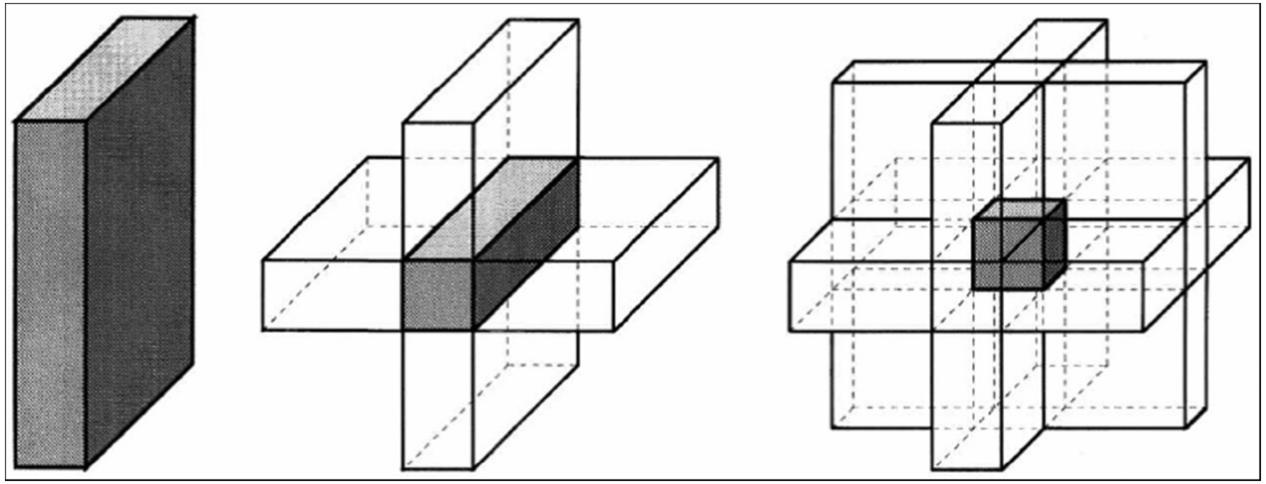

LOCALIZATION SEQUENCES

Non-echo	Echo formation based
Image Selected In vivo Spectroscopy (ISIS)	Stimulated Echo Acquisition Mode (STEAM)
Outer Volume Suppression (OVS)	Point RESolved Spectroscopy (PRESS)
	Semiadiabatic localization by adiabatic selective refocusing (sLASER)
	Semiadiabatic spin echo full intensity acquired localized spectroscopy (sSPECIAL)

for Short T2 metabolites

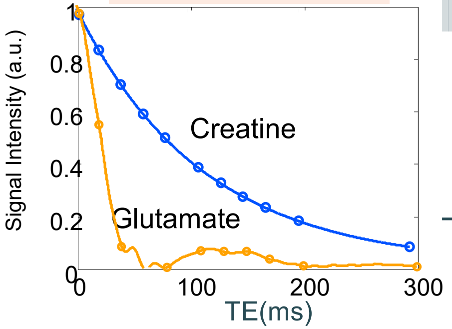

Short TE
Long TE for spectral editing

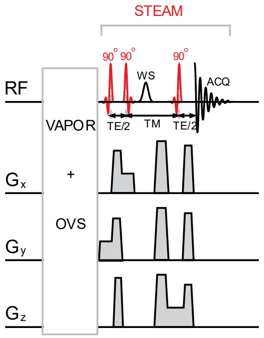

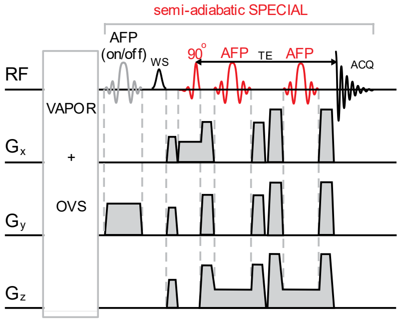

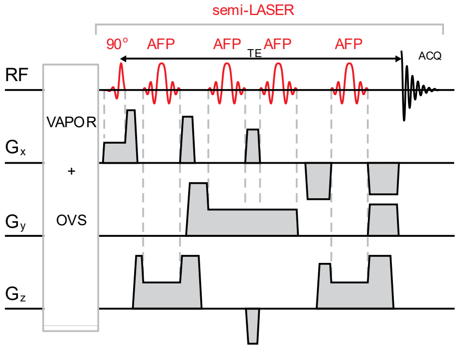

CHEMICAL SHIFT DISPLACEMENT (CSD) ERROR

Different resonances may experience different slice selection in the localization sequence due to limited excitation bandwidth of the RF pulses

CSDE (%): $\frac{\Delta x}{x} = \frac{\Delta f}{BW}$

e.g. 10% error along one axis
Origin VOI:
$1*1*1cm^3=1cm^3$
$0.9*0.9*0.9cm^3=0.73cm^3$

- Broadband RF pulse
- Strong gradient

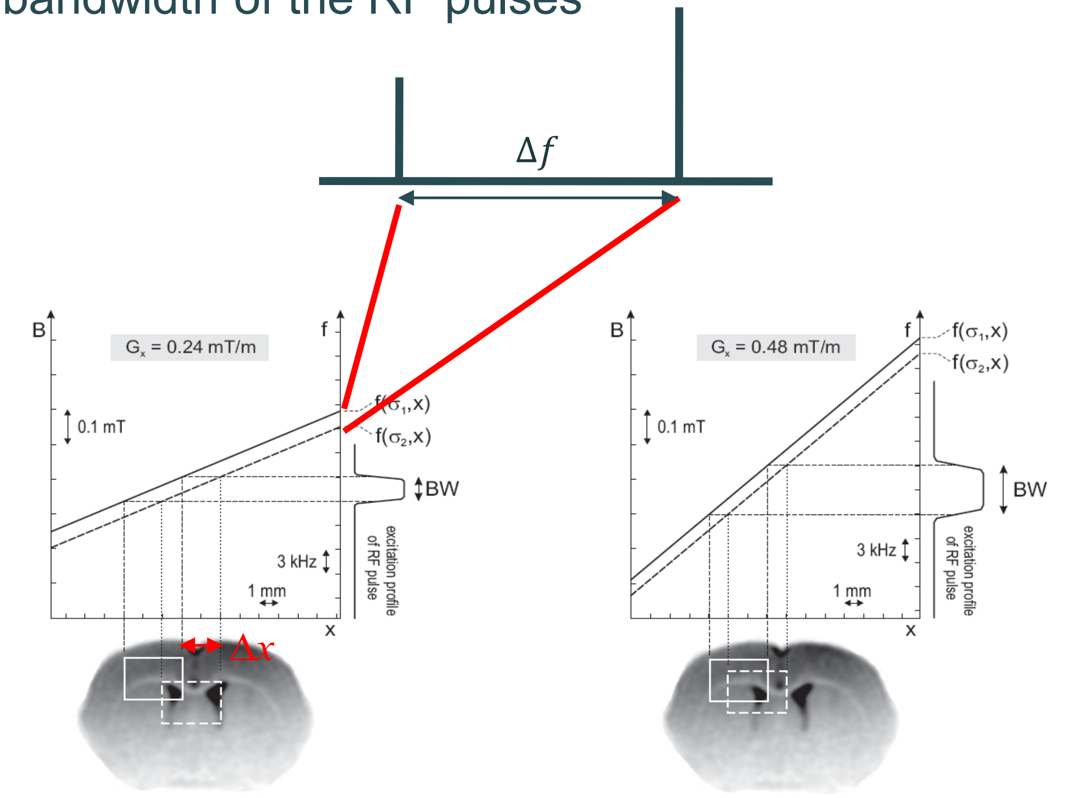

CIBM.CH

CSDE FOR J-COUPLED METABOLITES

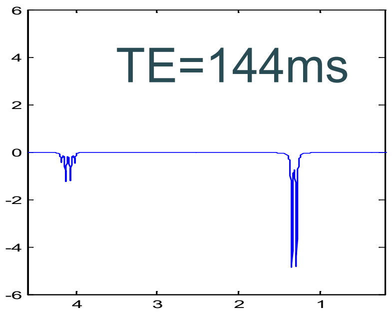

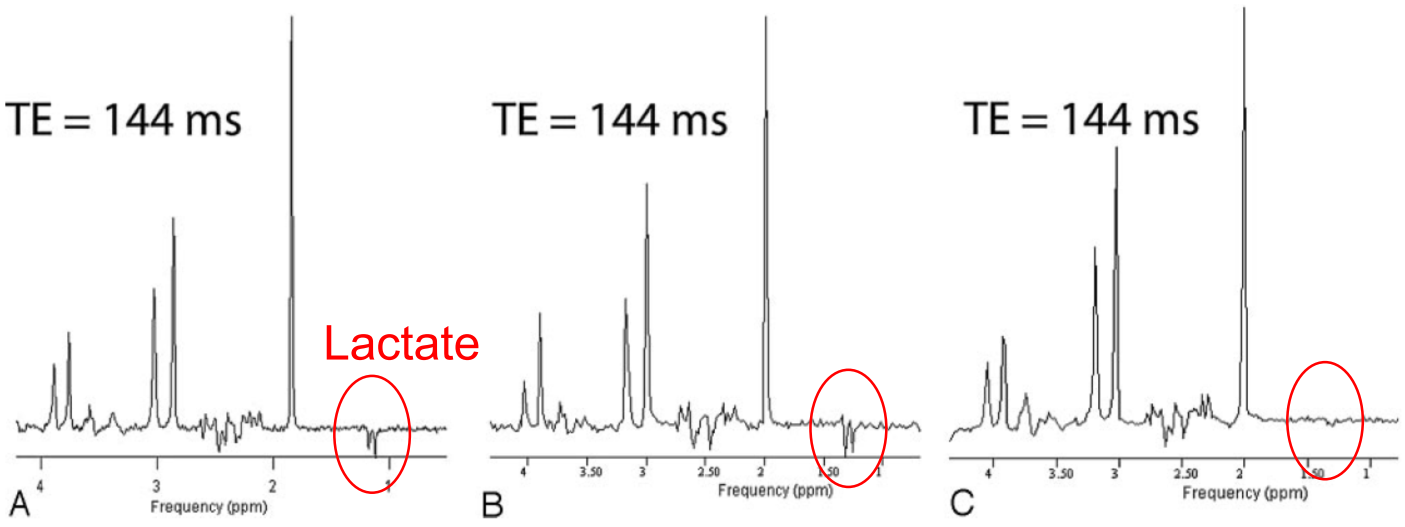

Radio-frequency pulse bandwidths for the selective refocusing pulses vary between vendors in the range of 874–2300 Hz.

Lange et al, Am J Neuroradiol 27,2006.

CSDE FOR J-COUPLED METABOLITES

Lactate

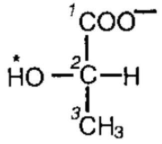

J=7Hz

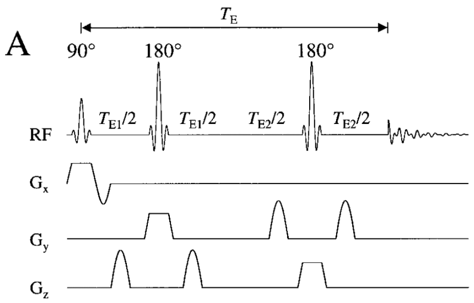

PRESS

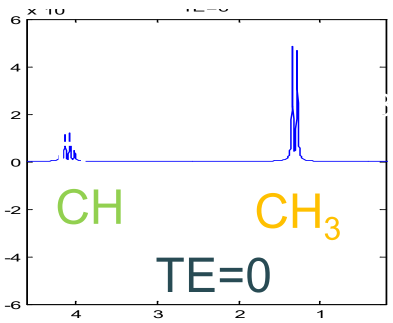

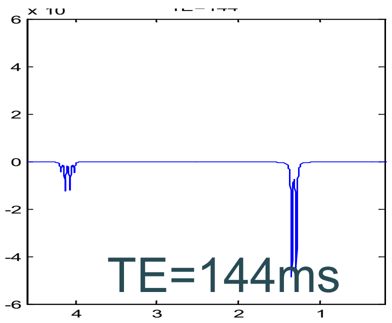

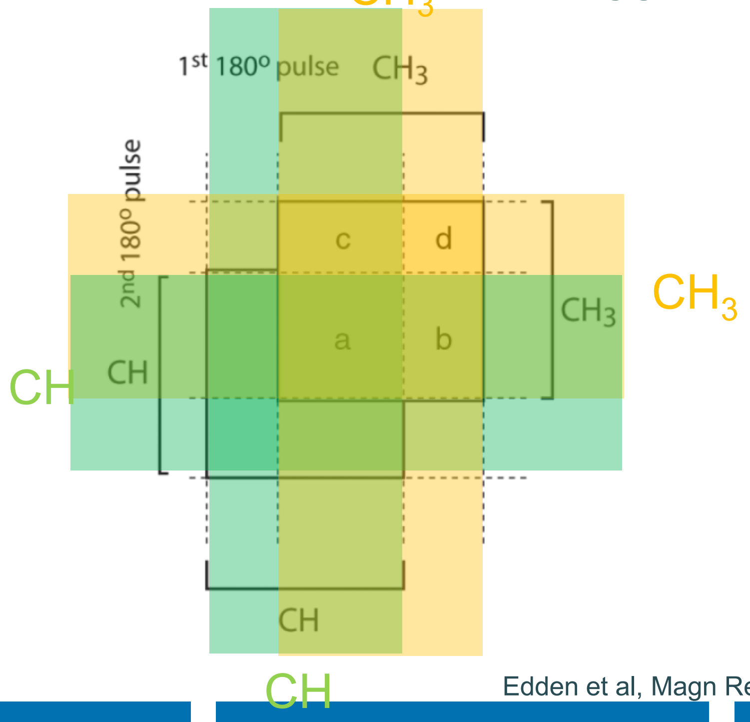

(CH3)

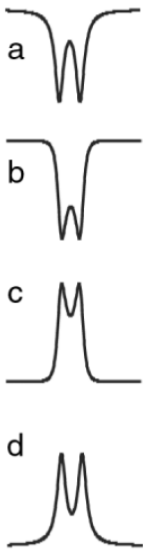

Edden et al, Magn Reson Med, 56, 2006

	CH	CH_3
a		80
b		80
c		80
d		80

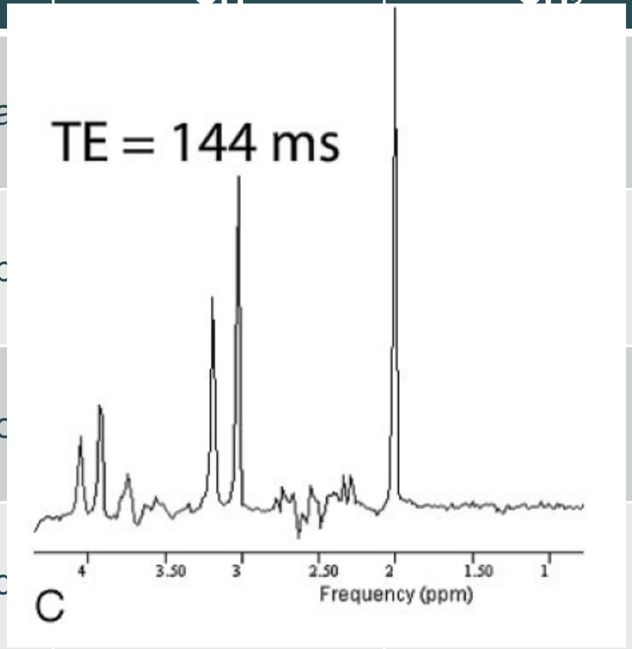

EXAMPLE OF CSDE IN MRSI

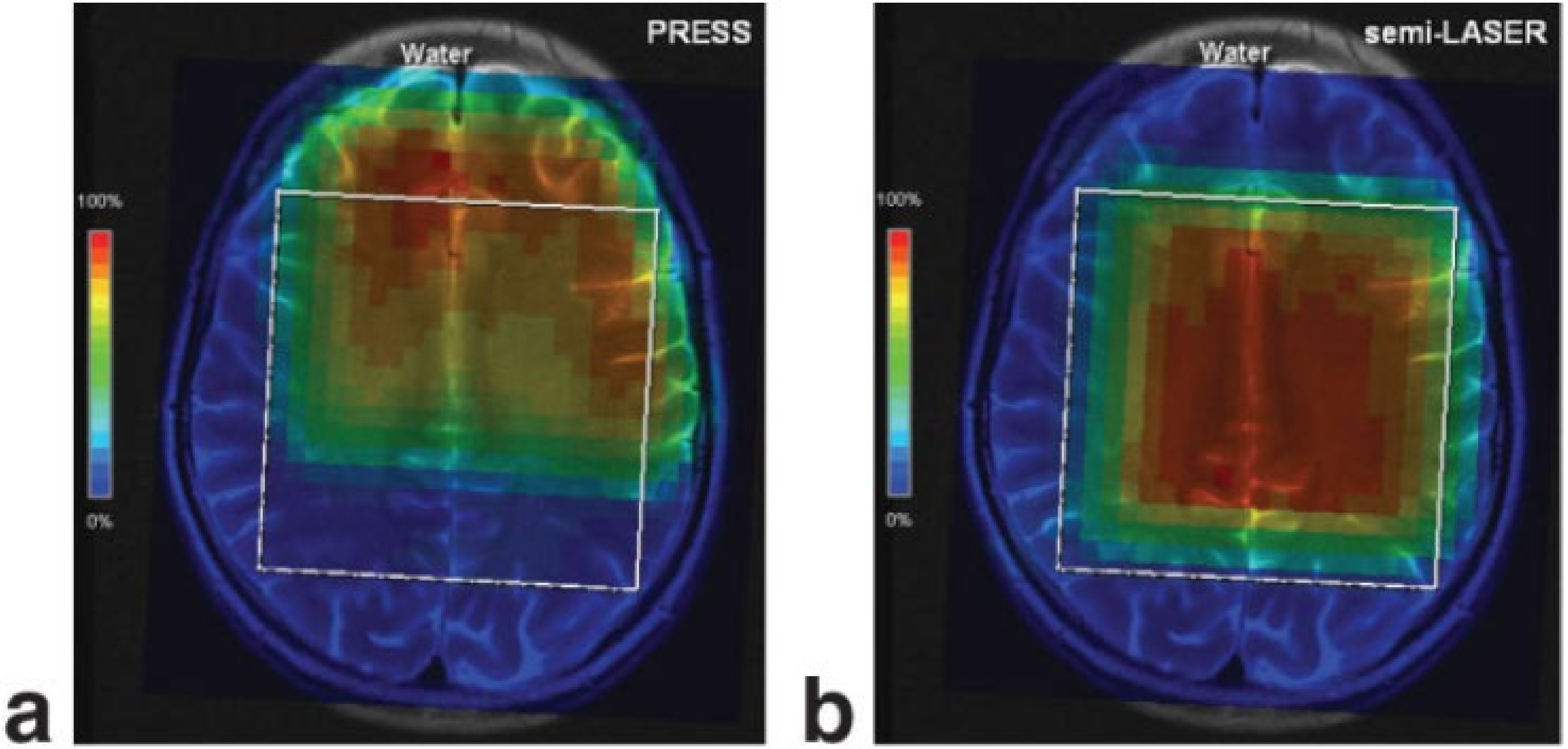

SUMMARY FOR REDUCING CSDE

CSDE (%): $\frac{\Delta x}{x} = \frac{\Delta f}{BW}$

- Broadband RF pulse
- Strong gradient

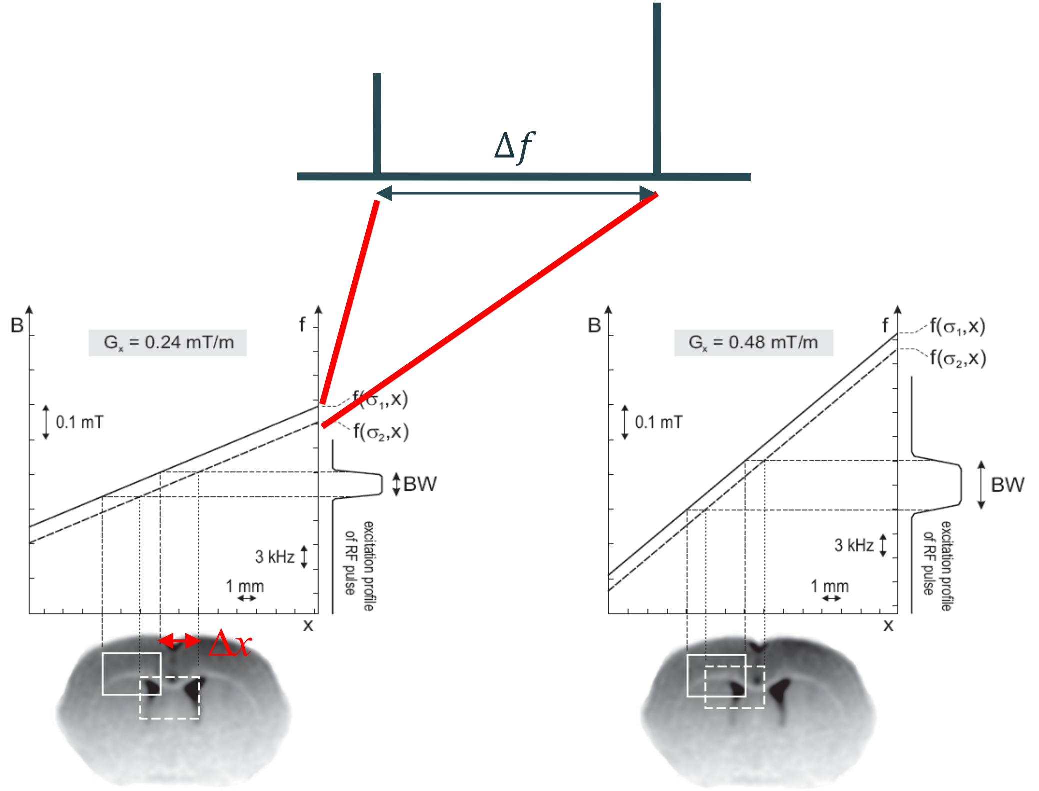

C I B M . C H

IMAGE SELECTED IN VIVO SPECTROSCOPY (ISIS)

Multiple scans with add/subtract scheme

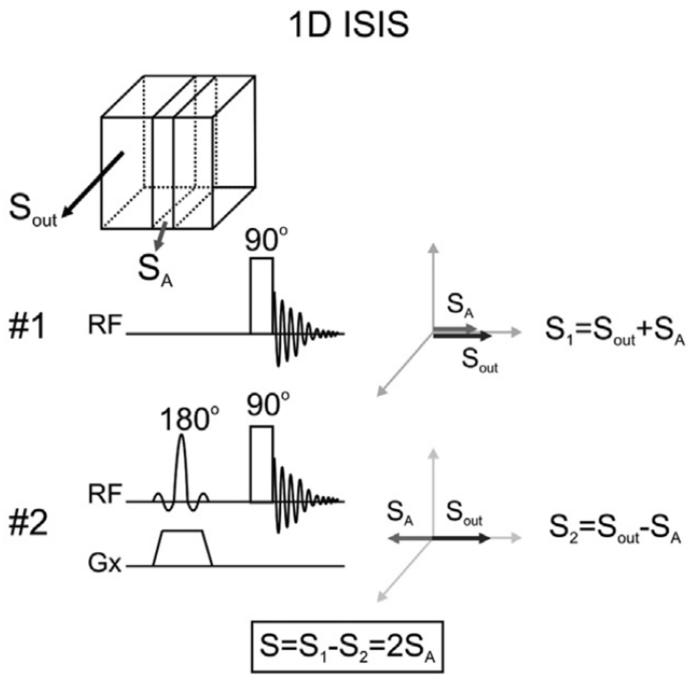

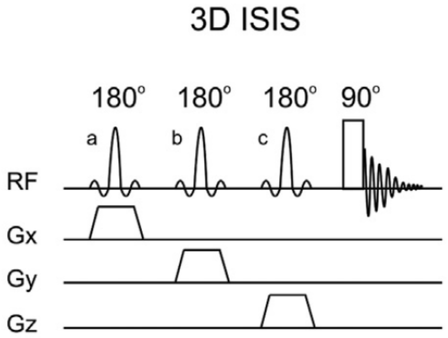

#	a	b	c	
1	OFF	OFF	OFF	+
2	ON	OFF	OFF	-
3	OFF	ON	OFF	-
4	OFF	OFF	ON	-
5	ON	ON	OFF	+
6	ON	OFF	ON	+
7	OFF	ON	ON	+
8	ON	ON	ON	-

- Pros
  - No signal loss due to T_2 and J-evolution
- Cons
  - Sensitive to motion during addition and subtraction
  - Signal loss due to T_1 relaxation

POINT-RESOLVED SPECTROSCOPY (PRESS)

Three slice-selective pulses form a double spin echo – one-shot technique

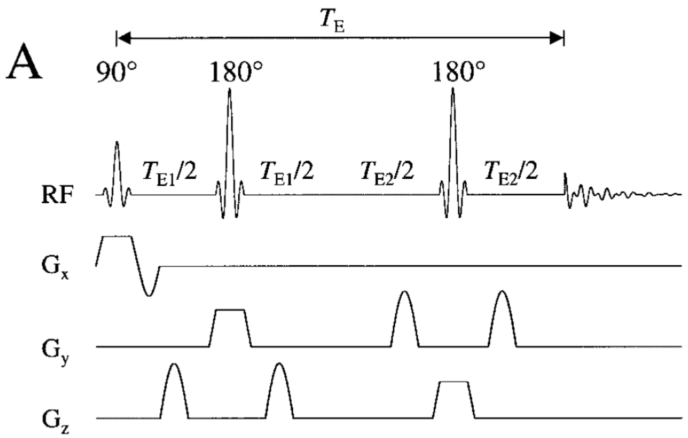

- Pros: - full signal intensity detected
  - insensitive to motion
- Cons: - rather long echo times
  - sufficient B_1 peak power necessary for 180° pulses

STIMULATED ECHO ACQUISITION MODE (STEAM)

Three slice-selective pulses form a stimulated echo – one-shot technique

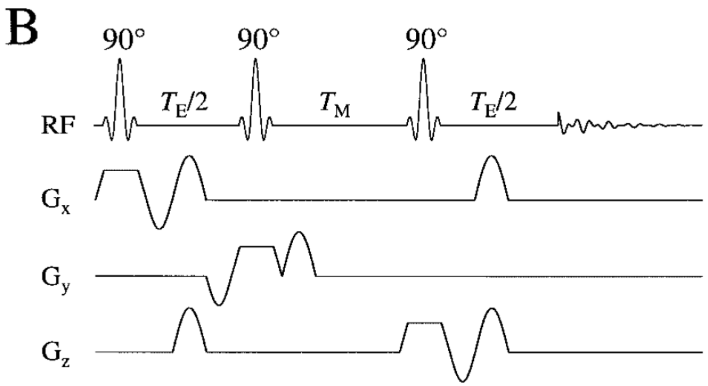

- Pros: - short echo time (relative to PRESS)
  - insensitive to motion
  - less sensitive to B_1 inhomogeneity than PRESS
- Cons: - only one half of the magnetization available

CIBM.CH

SLICE-SELECTIVE LOCALIZATION BY ADIABATIC SELECTIVE REFOCUSING (semi-LASER)

Slice-selective excitation + 2 pairs of slice-selective adiabatic refocusing pulses

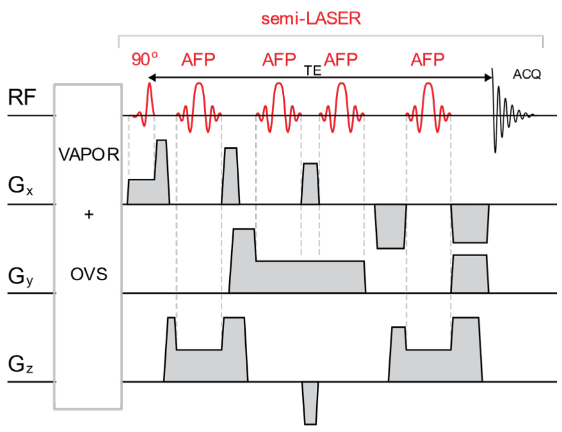

Adiabatic pulses generate a nonlinear phase variation across the slice and must be applied in pairs to obtain a slice-selective spin echo

- Pros: - full signal intensity available
  - longer minimum echo time but suppressed J-evolution
  - insensitive to B_1 inhomogeneity in two dimensions
- Cons: - Longer echo time leads to T_2 weighting of signal
  - high B_1 peak power necessary for 180° pulses

CIBM.CH

SEMI-ADIABATIC SPIN ECHO, FULL INTENSITY ACQUIRED LOCALIZED SPECTROSCOPY (sSPECIAL)

Spin-echo based add/subtract scheme - two shots technique

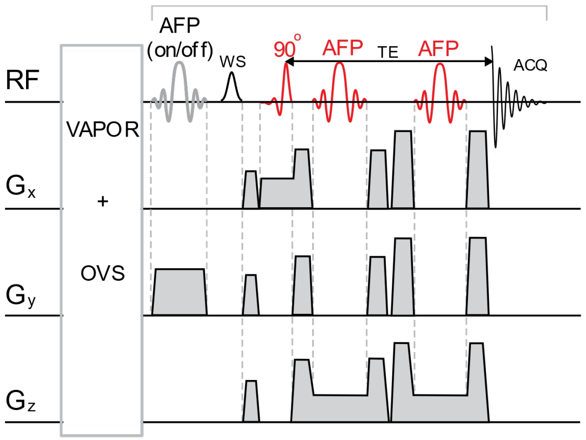

- Pros: - full signal intensity available
  - short TE (minimal signal loss due to T_2 and J-evolution)
  - insensitive to B_1 inhomogeneity in two dimensions
- Cons: - two scans necessary for localization
  - more sensitive to motion than single-shot methods
  - high B_1 peak power necessary for 180° pulses

CIBM.CH

B_0 SHIMMING

MAGNETIC FIELD INHOMOGENEITY

Ex vivo spectrum of brain extract

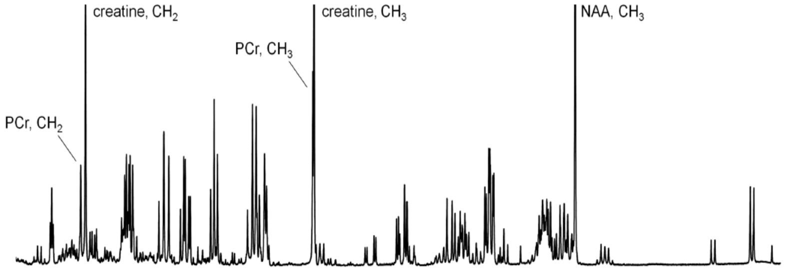

Anal. Chem. 83, 216–224 (2011)

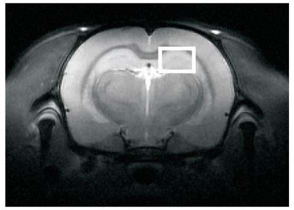

In vivo spectrum of a rat brain

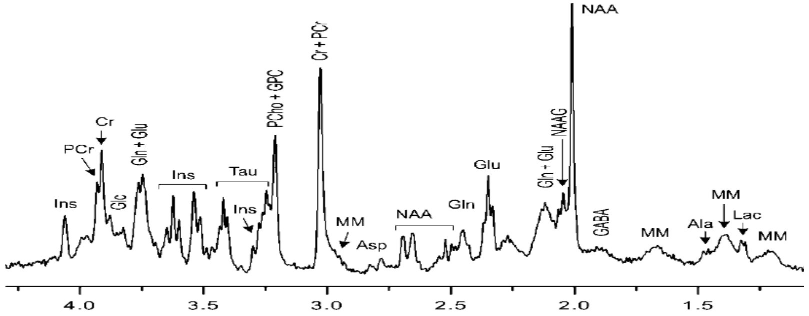

Magn Reson Med 41:649–656 (1999)

C I B M . C H

ORIGIN OF MAGNETIC FIELD INHOMOGENEITY

- magnetic susceptibility difference between air and tissue
  - Brain tissue(70-80% of water): diamagnetic
  - Oxygen: paramagnetic

e.g. prefrontal cortex (close to nasal sinus cavity, air-tissue surface)

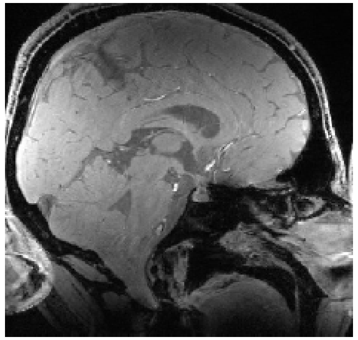

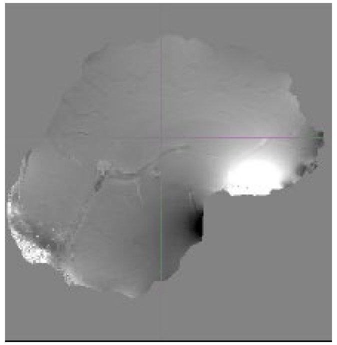

http://mriquestions.com

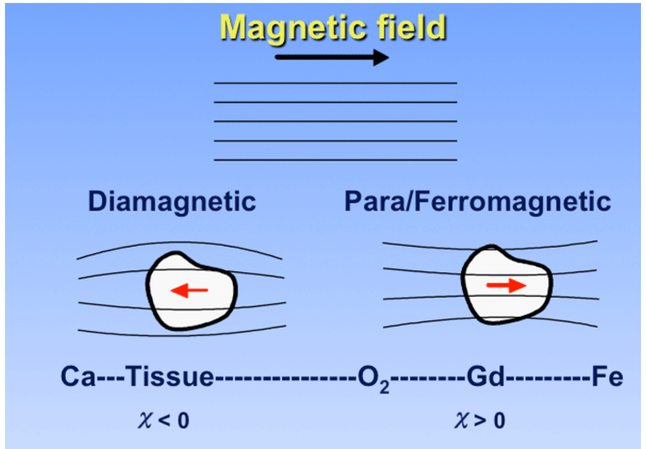

Water
Fat
tissues

O_2

MAGNETIC FIELD INHOMOGENEITY

Ex vivo spectrum of brain extract

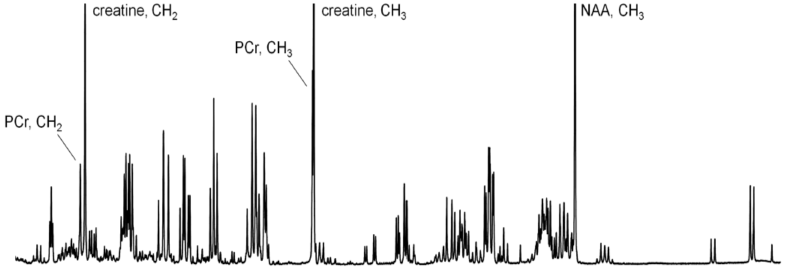

Anal. Chem. 83, 216–224 (2011)

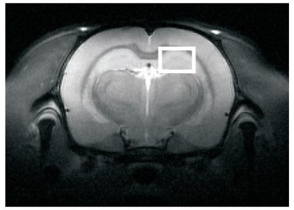

In vivo spectrum of a rat brain

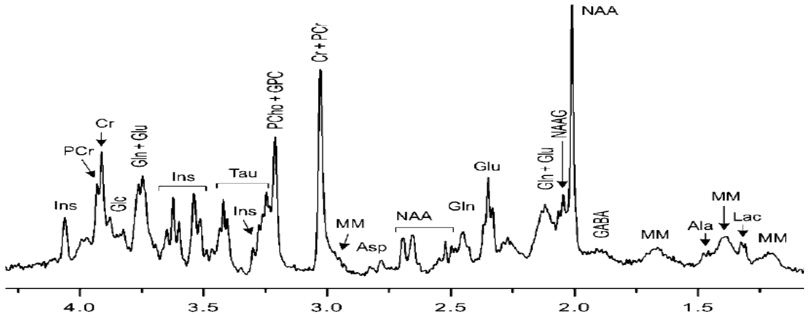

Magn Reson Med 41:649–656 (1999)

Higher magnetic susceptibility gradient in living tissue

C I B M . C H

B_0 SHIMMING: OPTIMIZE FIELD INHOMOGENEITY

Poor shimming!

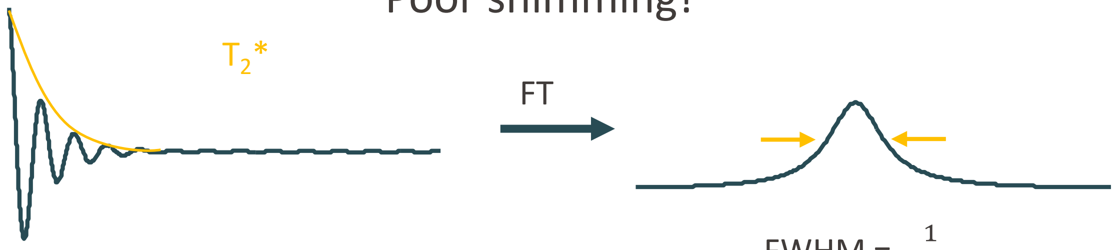

$\text{FWHM} = \frac{1}{\pi T_2{}^*}$

Time domain

Frequency domain

$$\downarrow FWHM \sim \frac{1}{\pi T_2^*} = \frac{1}{\pi T_2} + \frac{\gamma}{2\pi}\Delta B_0$$

Compensated by shimming

CIBM.CH

B_0 SHIMMING: OPTIMIZE FIELD INHOMOGENEITY

Better shimming!

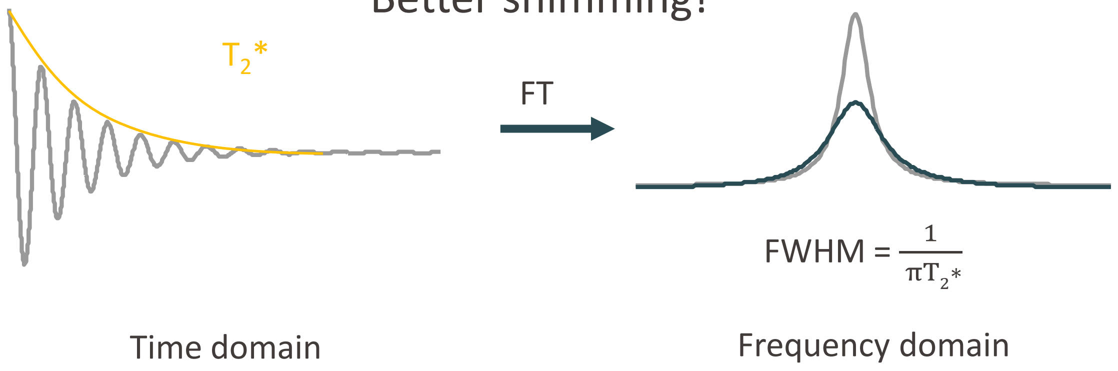

$$\downarrow FWHM \sim \frac{1}{\pi T_2^*} = \frac{1}{\pi T_2} + \frac{\gamma}{2\pi}\Delta B_0$$

Compensated by shimming

B_0 SHIMMING: OPTIMIZE FIELD INHOMOGENEITY

Great shimming!

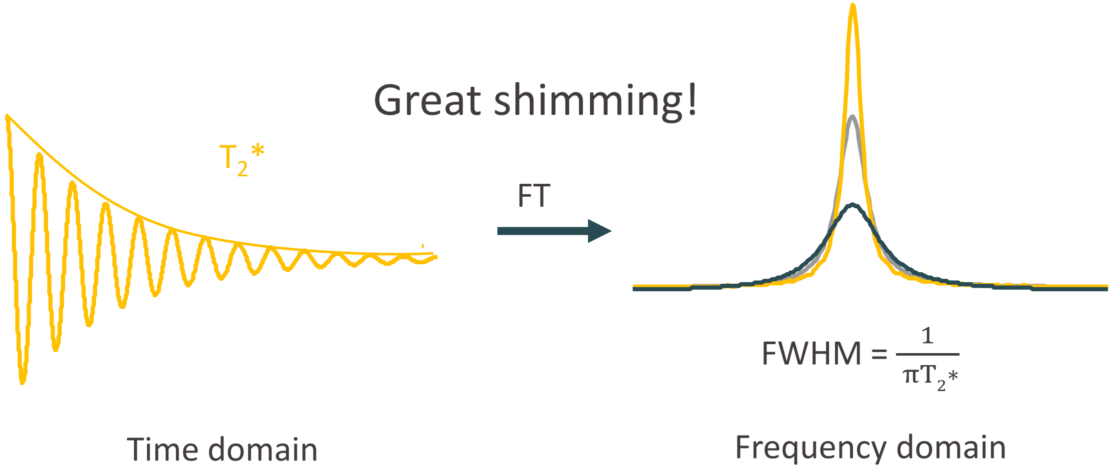

$$\downarrow FWHM \sim \frac{1}{\pi T_2^*} = \frac{1}{\pi T_2} + \frac{\gamma}{2\pi}\Delta B_0$$

Compensated by shimming

EFFECT OF B_0 INHOMOGENEITY ON SPECTRAL RESOLUTION

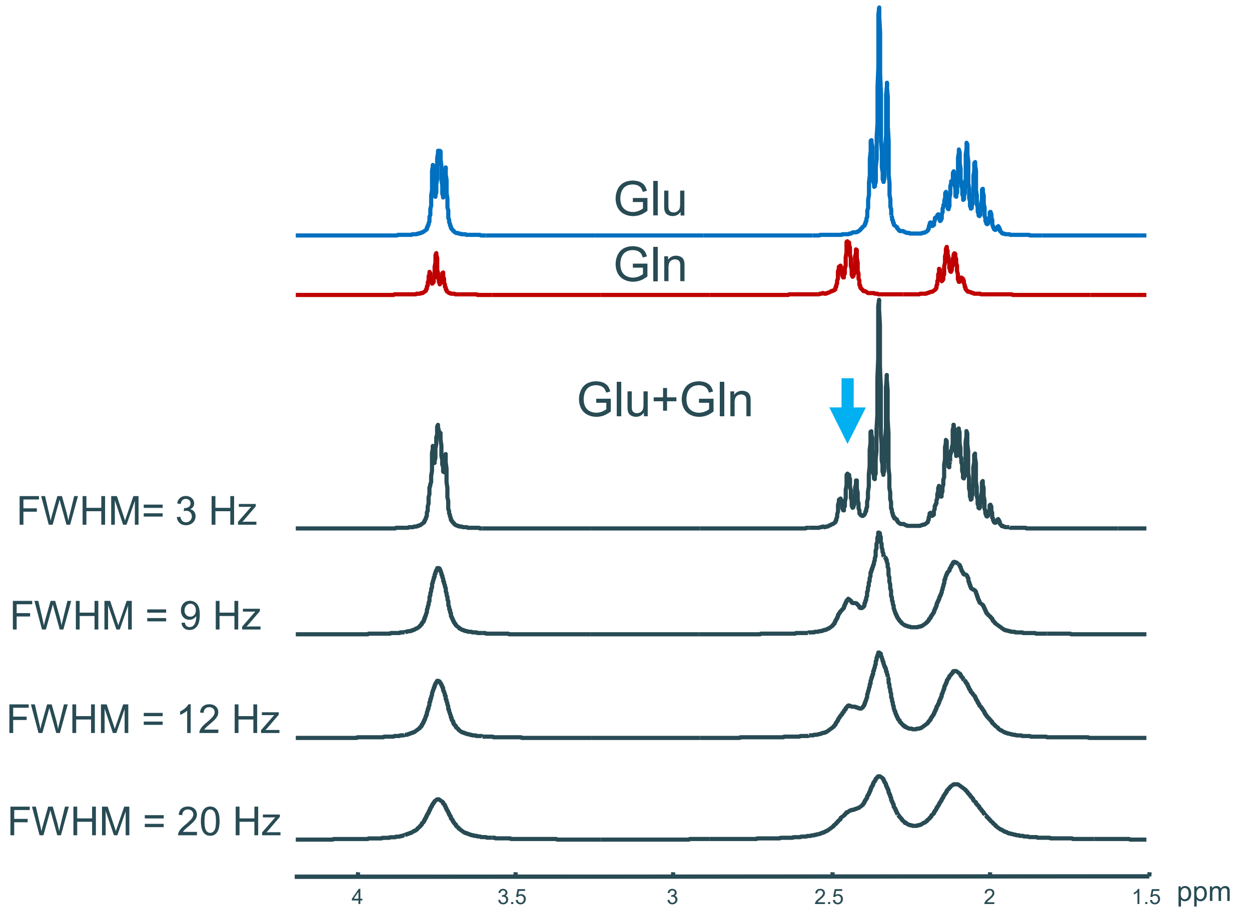

EFFECT OF B_0 INHOMOGENEITY ON SPECTRAL RESOLUTION

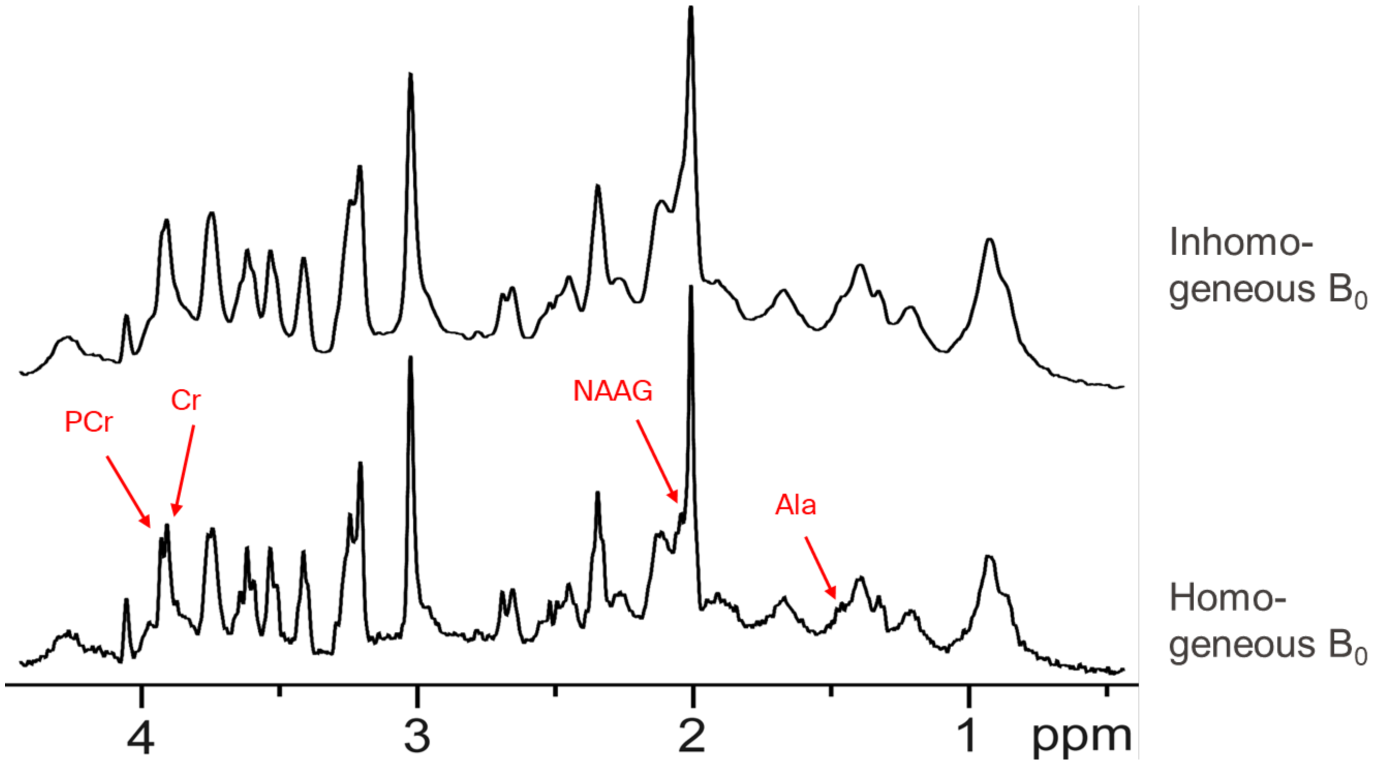

WHY: B_0 SHIMMING

- Improved SNR
- Improved spectral resolution
- Efficient water suppression, outer volume suppression and editing performance (especially for MRSI)
- Avoiding mislocalization and distortion of localization profile

Dotted line: frequency-position mapping without B0 inhomogeneities

Solid line: frequency-position mapping with superposition of metal induced field inhomogeneities

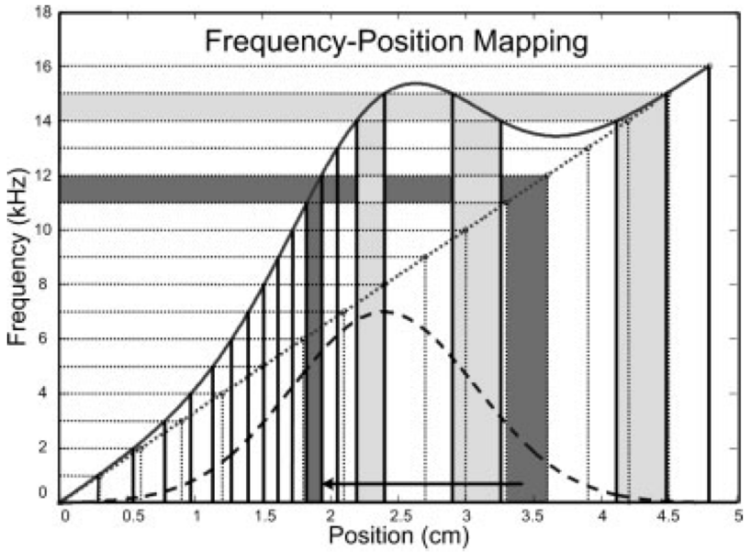

W. Lu et al. Magn Reson Med 62, 2009.

CIBM.CH

SPHERICAL HARMONICS FOR B_0 FIELD

- Magnetic field can be described as a linear combination of spherical harmonics

$$B_0(r,\theta,\phi) = \sum_n \left(r^n * \sum_i (k_{nm} * W_{nm}(\phi,\theta)) \right)$$

r : Vector to spatial location (x,y,z) in the magnet

$W_{nm}(\phi,\theta)$: Angular functions based on spherical harmonics

K_{nm} : Coefficients of expansion

ϕ,θ : fixed for a given projection

Field Generated by Low-Order Shims and Associated Spherical Harmonic Functions in Spherical and Cartesian Coordinates[a]

Order	n	m	Shorthand notation	Coefficients[b] (k_{nm})	Spatial dependence $r^n W_{nm}(\theta,\phi)$: Spherical	Spatial dependence $r^n W_{nm}(\theta,\phi)$: Cartesian	Coil type
1st order	1	0	Z^c	C_1	$r\cos\theta$	z	Gradient coils
	1	1	X^c	A_{11}	$r\sin\theta\cos\phi$	x	
	1	1	Y^c	B_{11}	$r\sin\theta\sin\phi$	y	
2nd order	2	0	Z^{2c}	C_2	$r^2(3\cos^2\theta - 1)/2$	$z^2\text{-}(x^2+y^2)/2$	Shim coils
	2	1	XZ	$3A_{21}$	$r^2\sin\theta\cos\theta\cos\phi$	xz	
	2	1	YZ	$3B_{21}$	$r^2\sin\theta\cos\theta\sin\phi$	yz	
	2	2	$X^2 - Y^{2c}$	$3A_{22}$	$r^2\sin^2\theta\cos 2\phi$	$x^2 - y^2$	
	2	2	$2XY$	$3B_{22}$	$r^2\sin^2\theta\sin 2\phi$	$2xy$	
3rd order	3	0	Z^3	C_3	$r^3(5\cos^3\theta - 3\cos\theta)/2$	$z[z^2 - 3(x^2+y^2)/2]$	Shim coils
	3	1	XZ^2	$\frac{3}{2}A_{31}$	$r^3\sin\theta(5\cos^2\theta - 1)\cos\phi$	$x(4z^2 - x^2 - y^2)$	
	3	1	YZ^2	$\frac{3}{2}B_{31}$	$r^3\sin\theta(5\cos^2\theta - 1)\sin\phi$	$y(4z^2 - x^2 - y^2)$	
	3	2	$Z(X^2 - Y^2)$	$15A_{32}$	$r^3\sin^2\theta\cos\theta\cos 2\phi$	$z(x^2 - y^2)$	
	3	2	XYZ	$15B_{32}$	$r^3\sin^2\theta\cos\theta\sin 2\phi$	$2xyz$	
	3	3	X^3	$15A_{33}$	$r^3\sin^3\theta\cos 3\phi$	$x^3 - 3xy^2$	
	3	3	Y^3	$15B_{33}$	$r^3\sin^3\theta\sin 3\phi$	$3x^2y - y^3$	

Gruetter et al, JMR,96 (1992)

SHIM COILS

Each shim coil produces magnetic field corresponding to one spherical harmonic field.

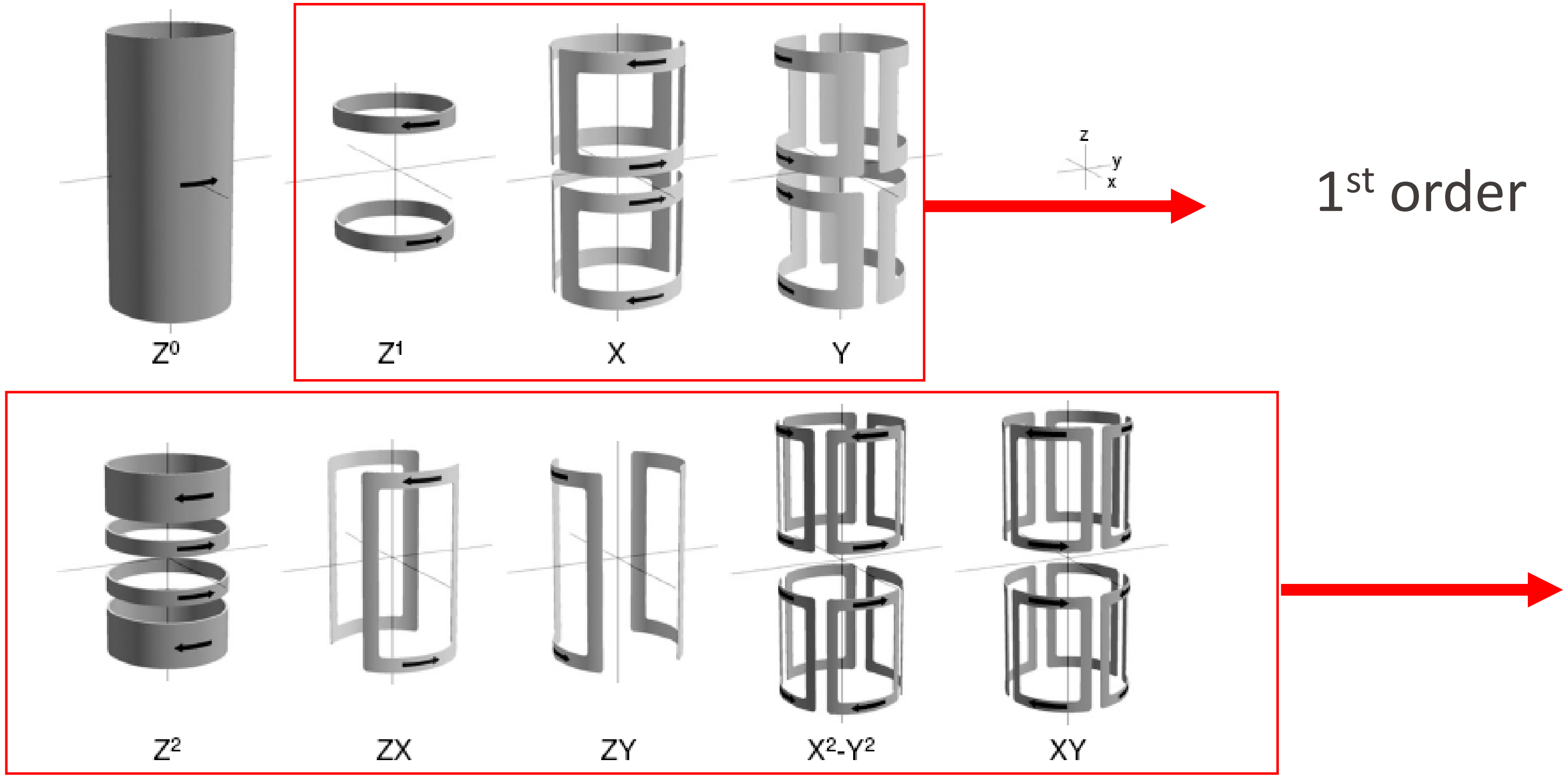

1^{st} order

2^{nd} order

de Graaf R. In Vivo NMR Spectroscopy: Principles and Techniques.1998.

B_0 SHIMMING METHODS

- B_0 can be measured from the **phase differences** of magnetization during a given period of free precession

- Manual shimming
  - Time-consuming

- Automated shimming methods (quantitative, accurate and fast)
  - 3D field mapping
  - projection based mapping: e.g. FASTMAP (high spatial sampling, preferred for small volume optimization)

Experiment 1: M(0)

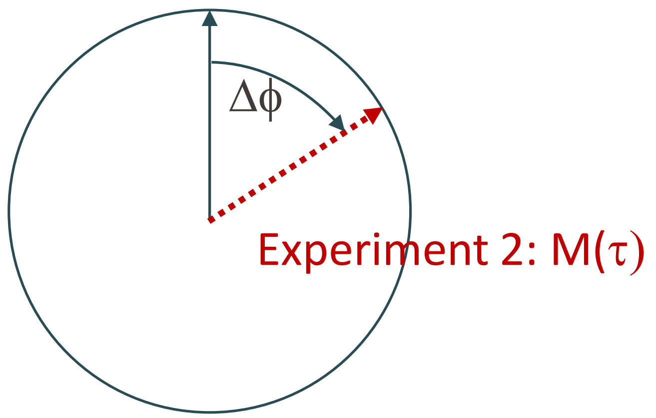

$$\Delta\phi^{(j)}(r,\tau) = \gamma B_0(r,\theta^{(j)},\phi^{(j)})\tau$$

EXAMPLE OF IN VITRO WATER SHIMMING RESULTS

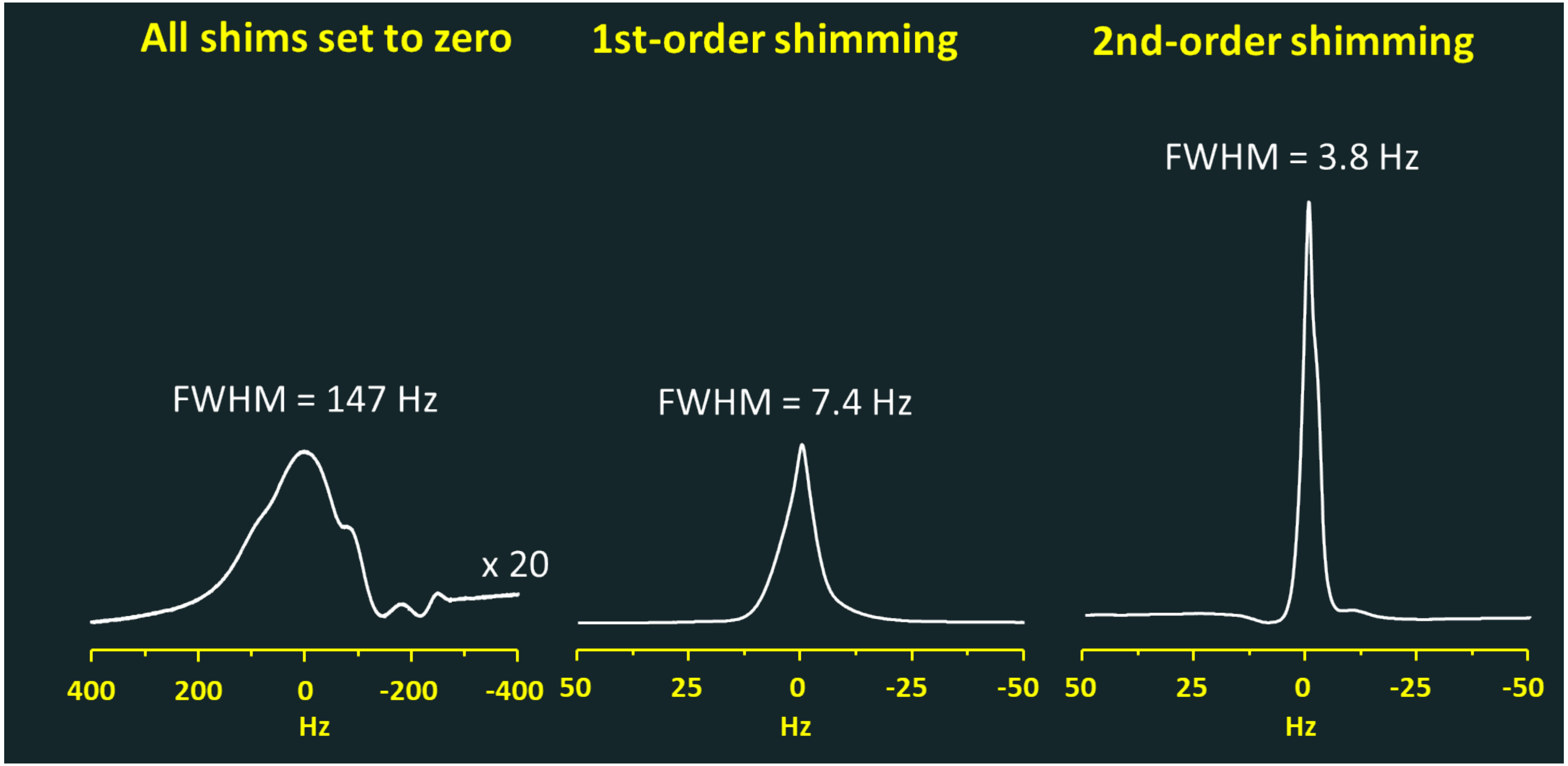

Tkac, University of Minnesota

Effect of 2nd-order shimming at 7 T

STEAM TE = 6 ms, VOI = 2 x 2 x 2 cm^3, occipital lobe, FASTMAP shimming

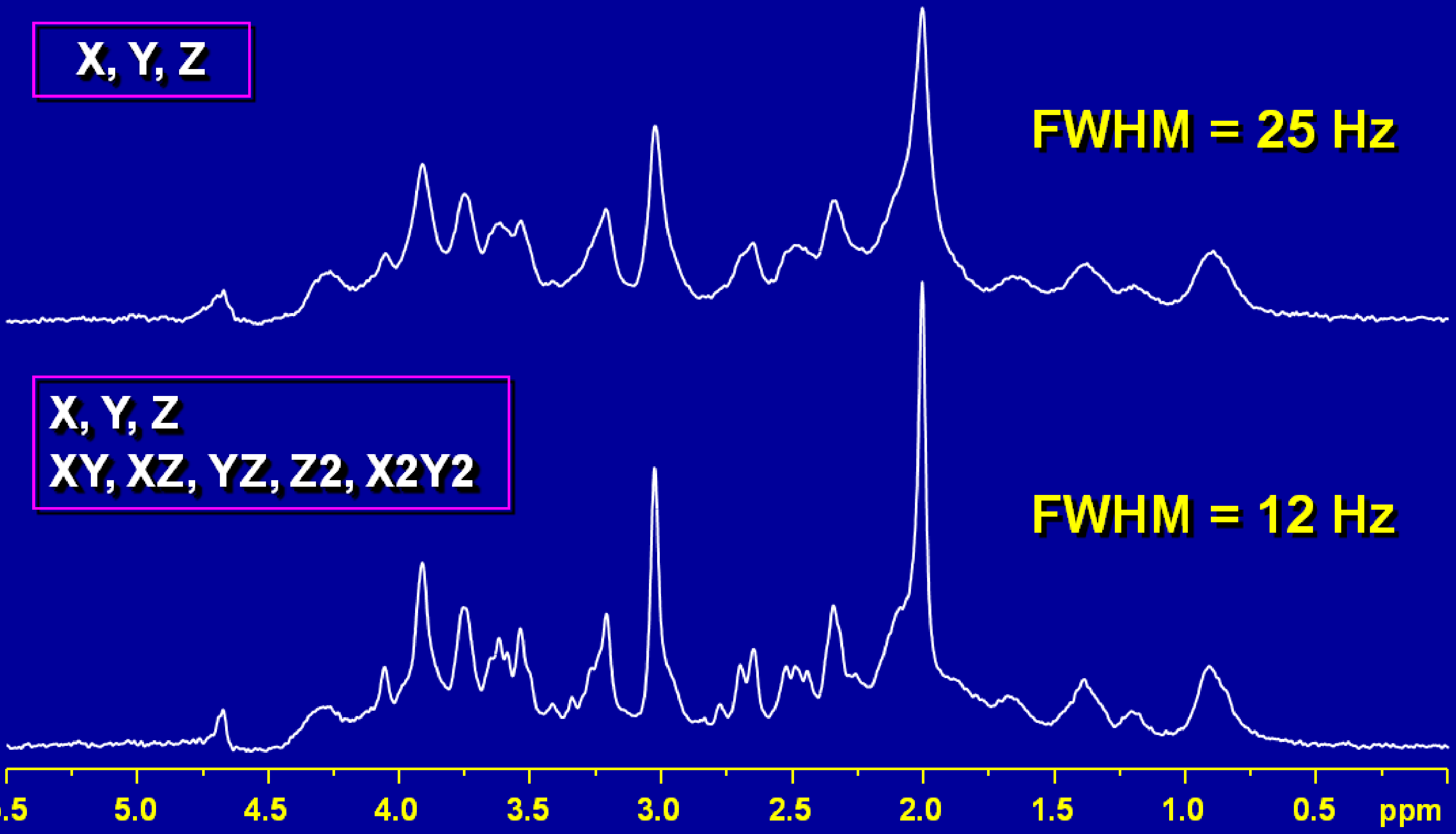

Tkac, University of Minnesota

B_1 CALIBRATION

B_1^+ CALIBRATION

- Why?
  - Achieve the required flip angle $\alpha = \gamma B_1 T$
  - Maximal signal intensity
  - Optimal slice profile to reach the best localization performance

- B_1^+ Calibration is critical before each scan
  - Different B_1 distribution for different subjects and coils

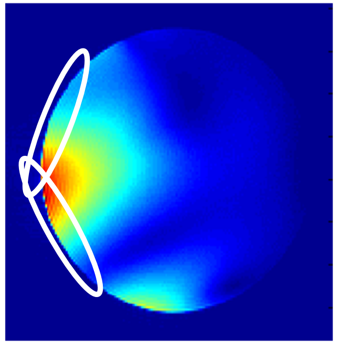

B_1^+ CALIBRATION

- Flip angle calibration $\alpha = \gamma B_1 T$

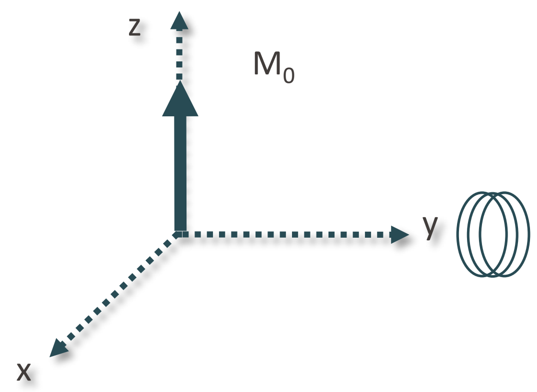

B_1^+ CALIBRATION

- Flip angle calibration $\alpha = \gamma B_1 T$

SI = $\sin(\alpha)$

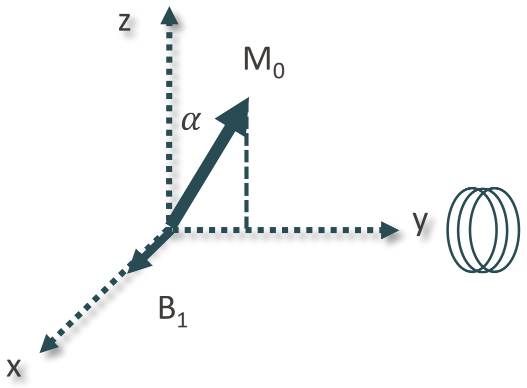

CIBM.CH

B_1^+ CALIBRATION

- Flip angle calibration $\alpha = \gamma B_1 T$

SI = $\sin(\alpha)$

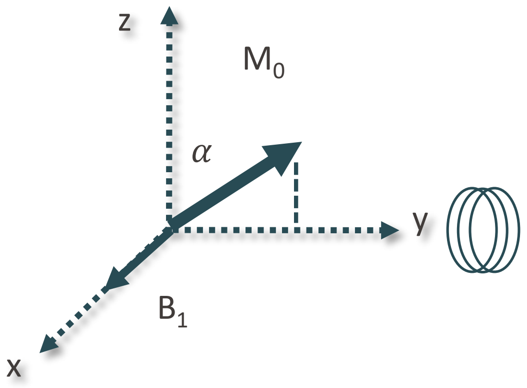

B_1^+ CALIBRATION

- Flip angle calibration $\alpha = \gamma B_1 T$

SI = $\sin(\alpha)$

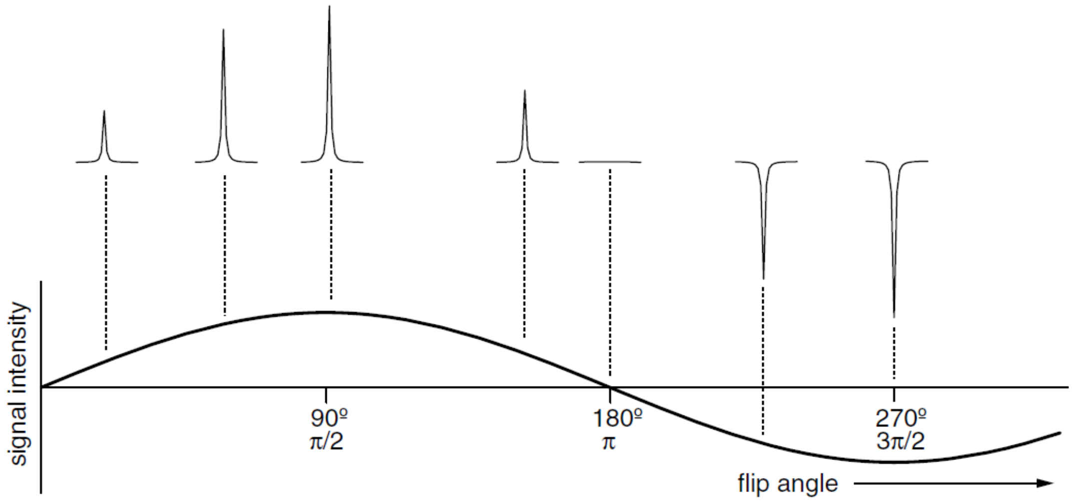

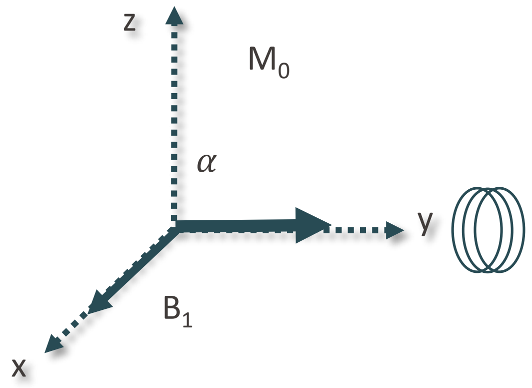

Keeler, Understanding NMR Spectroscopy,2002

B_1^+ CALIBRATION

- **Surface coil**
  - Calibrate local RF power for B_1^+

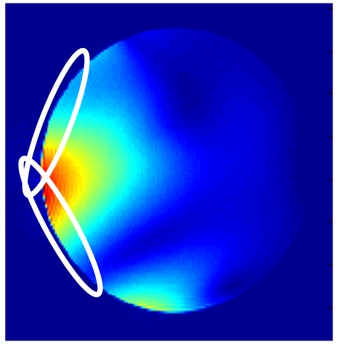

- **Volume coil**
  - Destructive and constructive interferences from standing waves at high magnetic fields (RF wavelength ≤ sample size) lead to inhomogeneous B_1 distribution
  - High permittivity dielectric pad
  - B_1^+ shimming using transmit arrays is desirable to achieve maximal local B_1^+

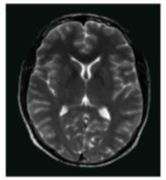

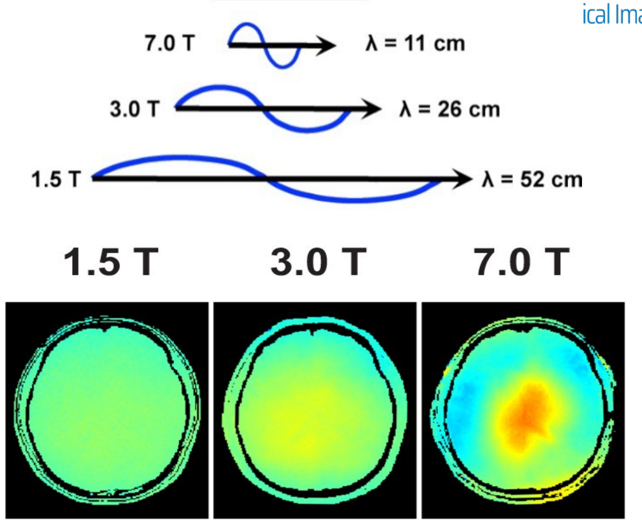

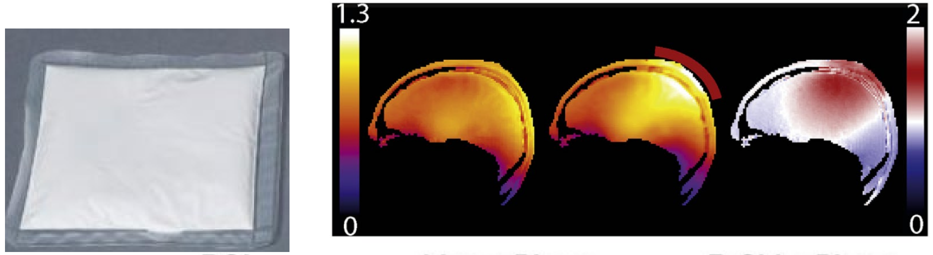

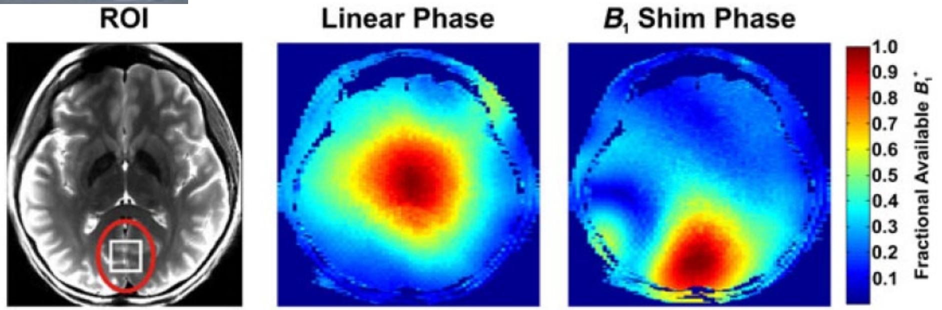

Emir et al., NMR Biomed., 2011; PLOS One, 2014 Mar 12;9(3):e91318. MRIquestions.com

WATER SUPPRESSION

WHY SUPPRESS WATER

- Water is about 10000 times bigger than metabolites
- Vibration induced water sidebands
- Baseline distortion

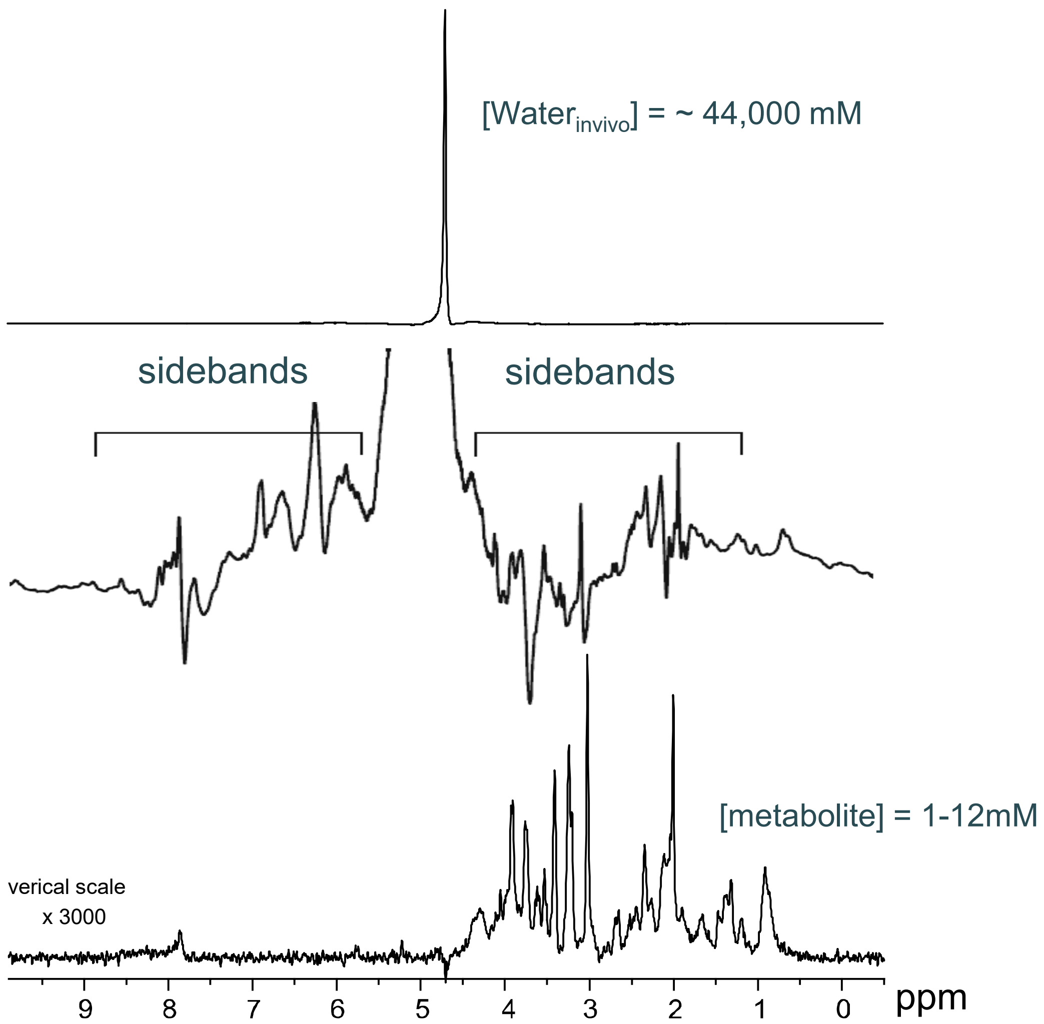

de Graaf R.A. (2012) Principles of 1H NMR Spectroscopy In Vivo. In: Choi IY., Gruetter R. (eds) Neural Metabolism In Vivo.

WATER SUPPRESSION MODULE

CHEmical Shift-Selective (CHESS)

Frequency selective pulse for water resonance

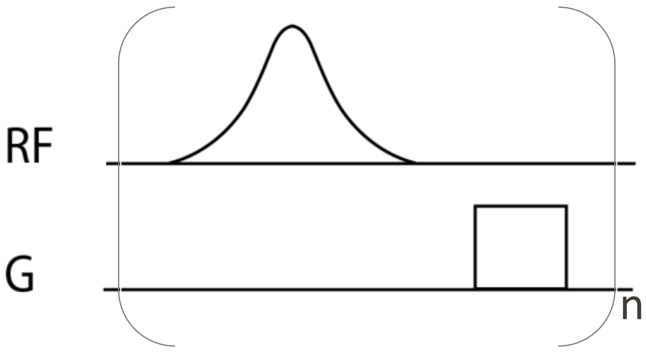

Spoiling gradient

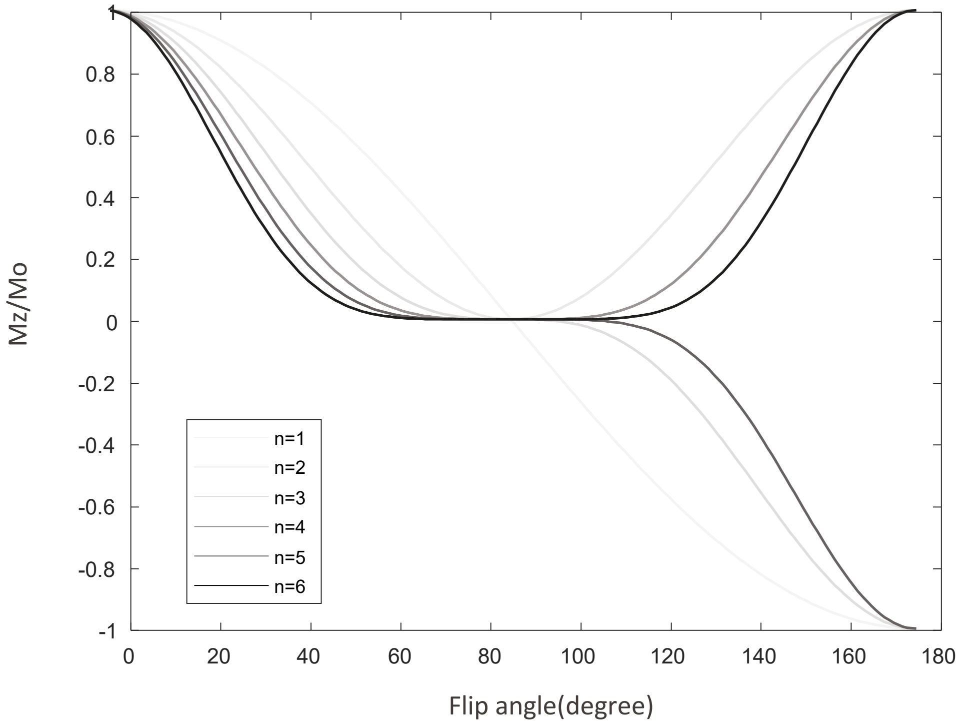

CIBM.CH

A Haase et al 1985 Phys. Med. Biol. 30 341

VAriable pulse Power and Optimized Relaxation delays (VAPOR)

- Multiple CHESS
- Variable delays
- Variable flip angles

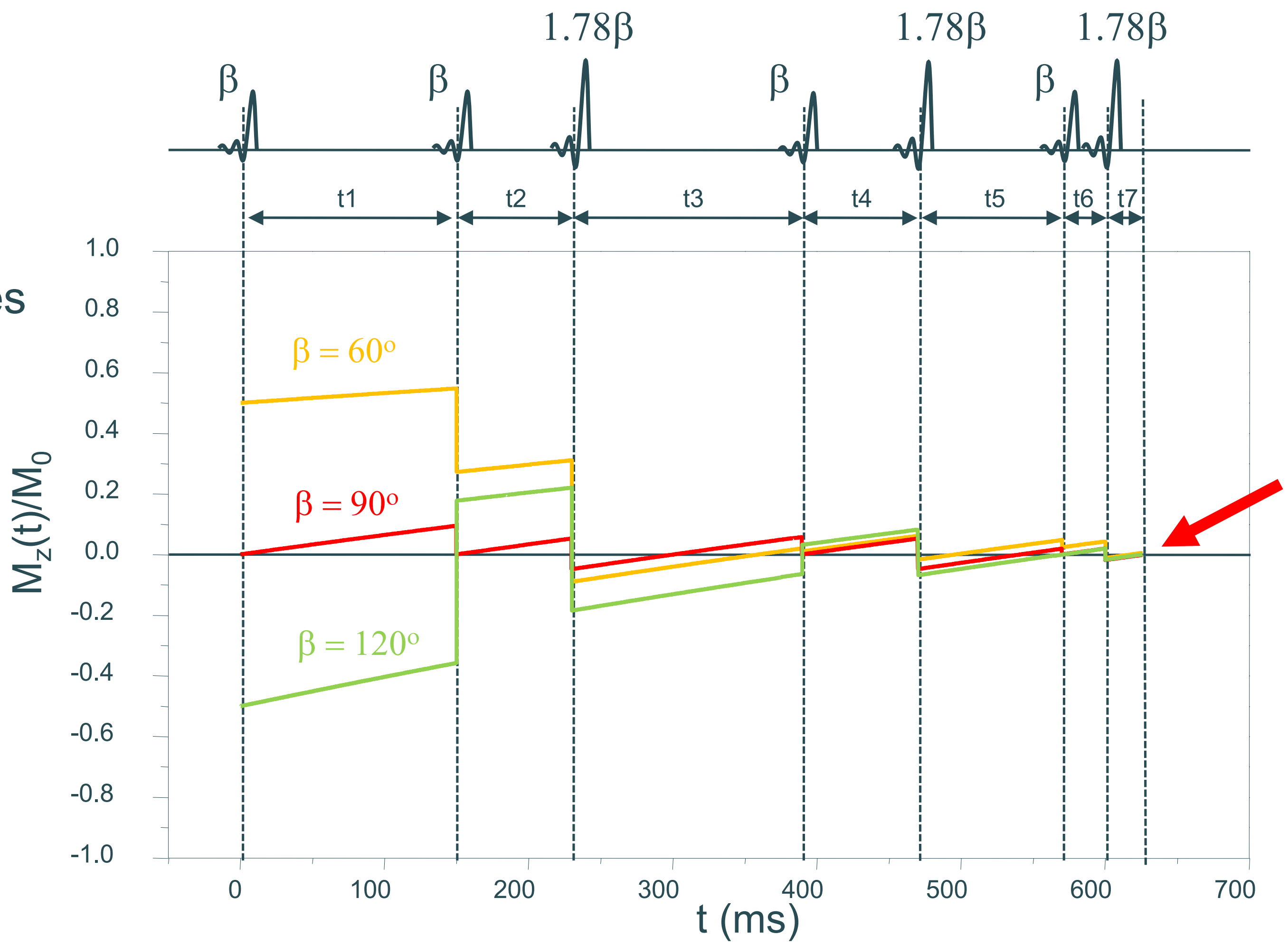

water Mz =0
prior to localization

Tkac et al., Magn Reson Med 1999

COMPARISON WITH OTHER WATER SUPPRESSION METHODS

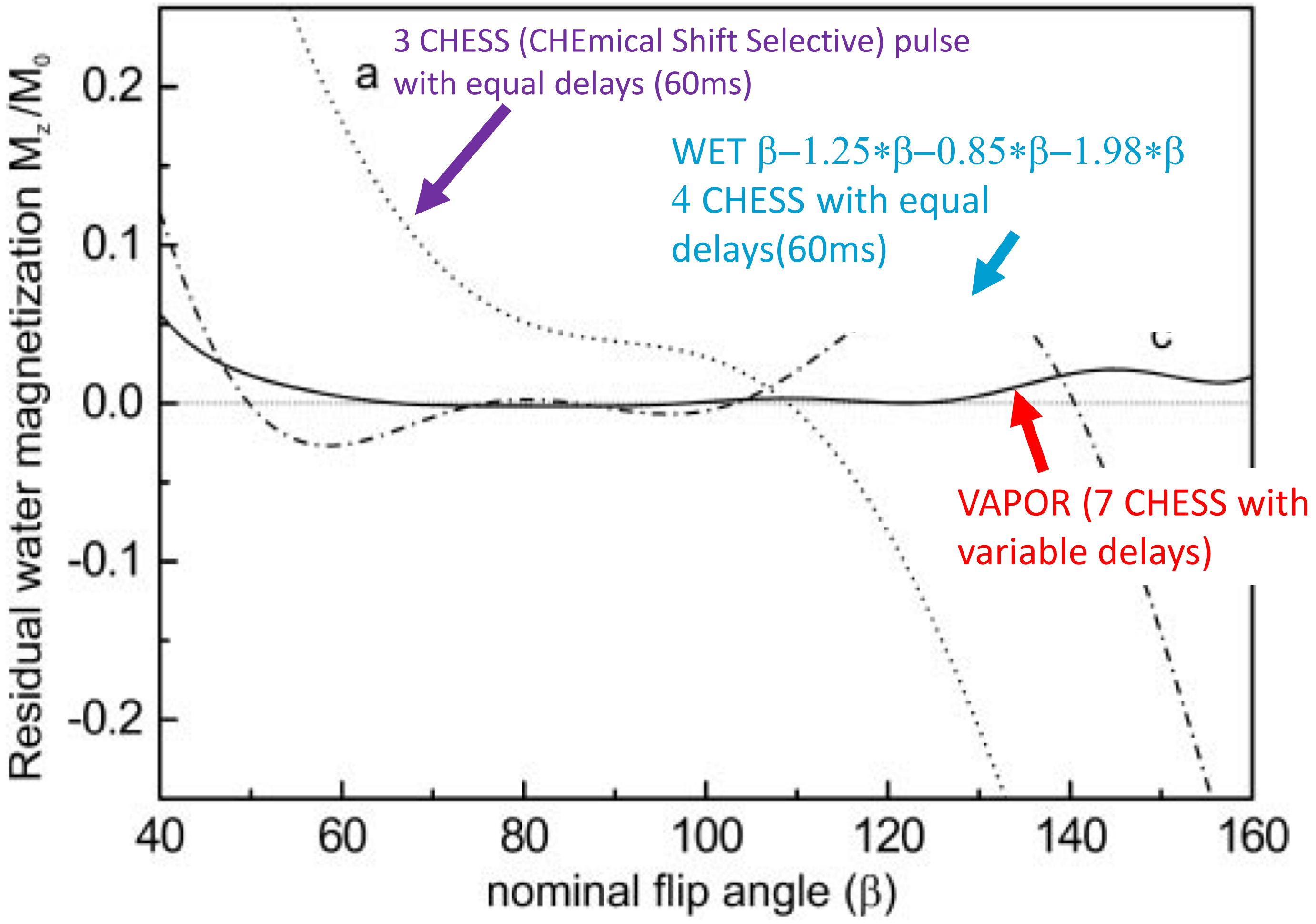

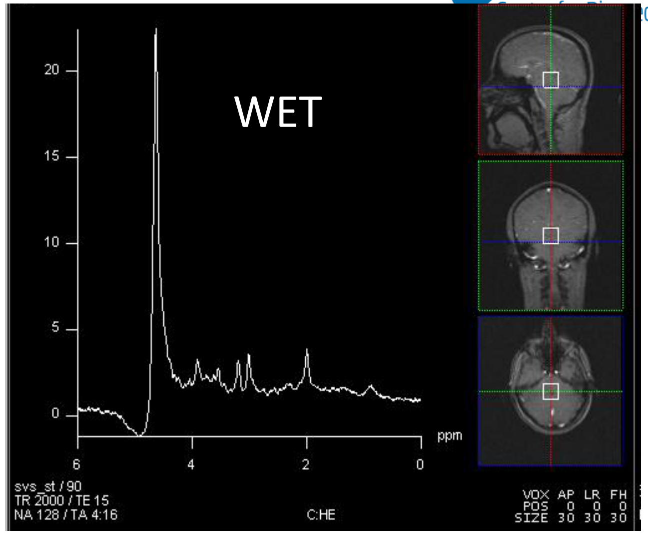

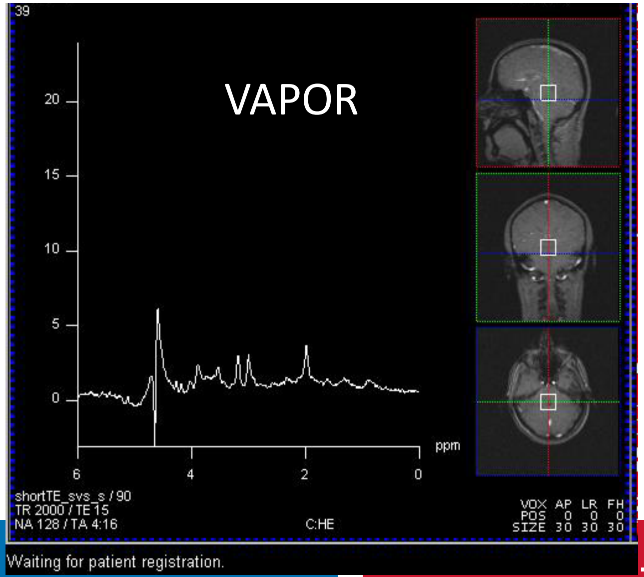

OUTER VOLUME SUPPRESSION

OUTER VOLUME SUPPRESSION (OVS)

Sinc pulse

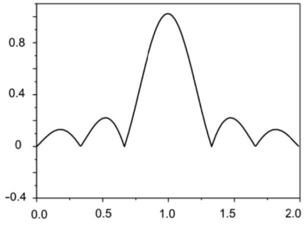

Imperfect slice profile

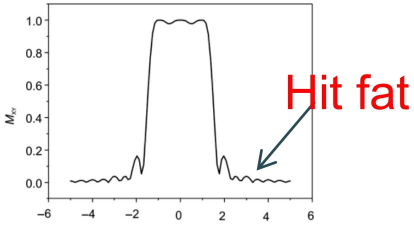

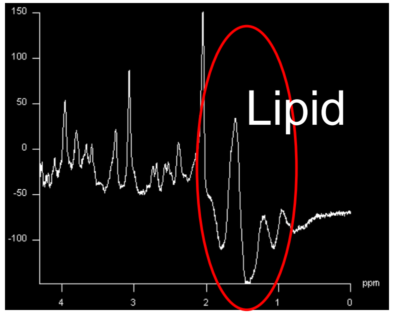

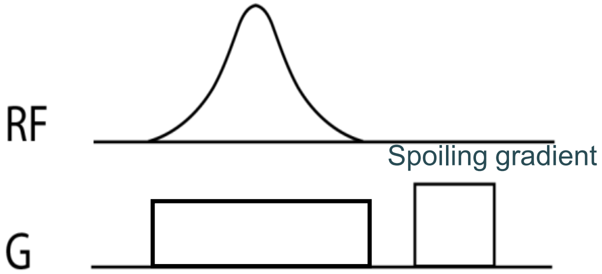

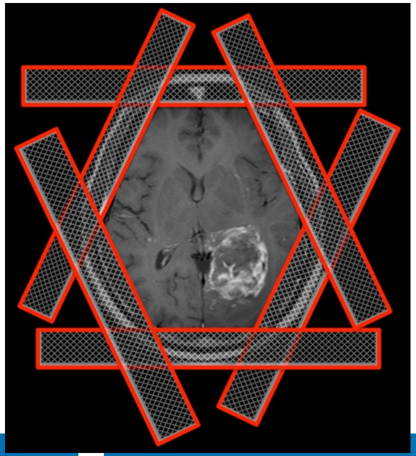

Spurious echo

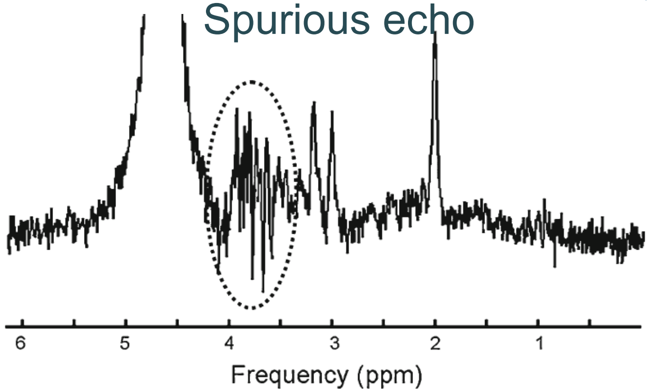

Water from elsewhere

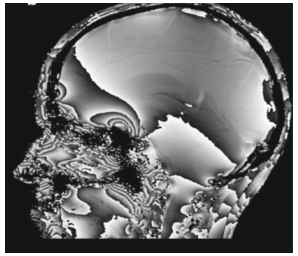

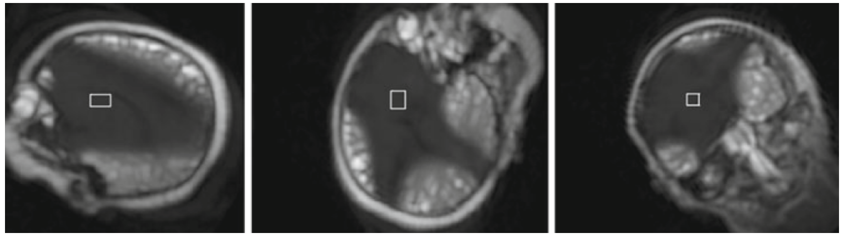

mriquestions.com; Carlsson et al.,Magn Reson Mater Phy 24, 2011.

CIBM
Center for Biomedical Imaging

C I B M . C H

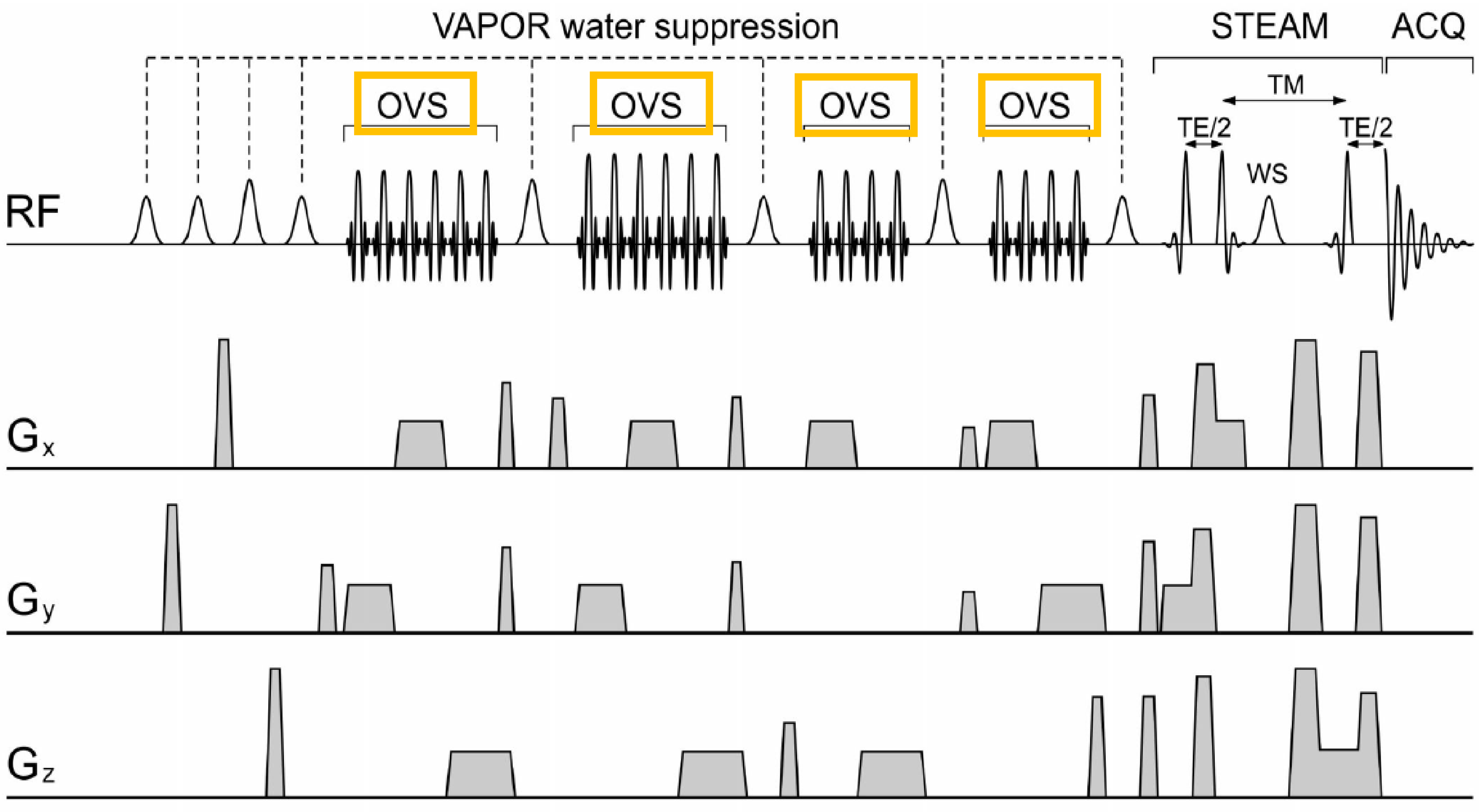

Application of several blocks of slice selective pulses saturating regions adjacent to the VOI. For a surface RF coil, variable amplitudes of the saturation pulses are useful.

Tkac et al., Appl Magn Reson, 2005

FINALLY, MR SPECTRUM QUALITY CONTROL

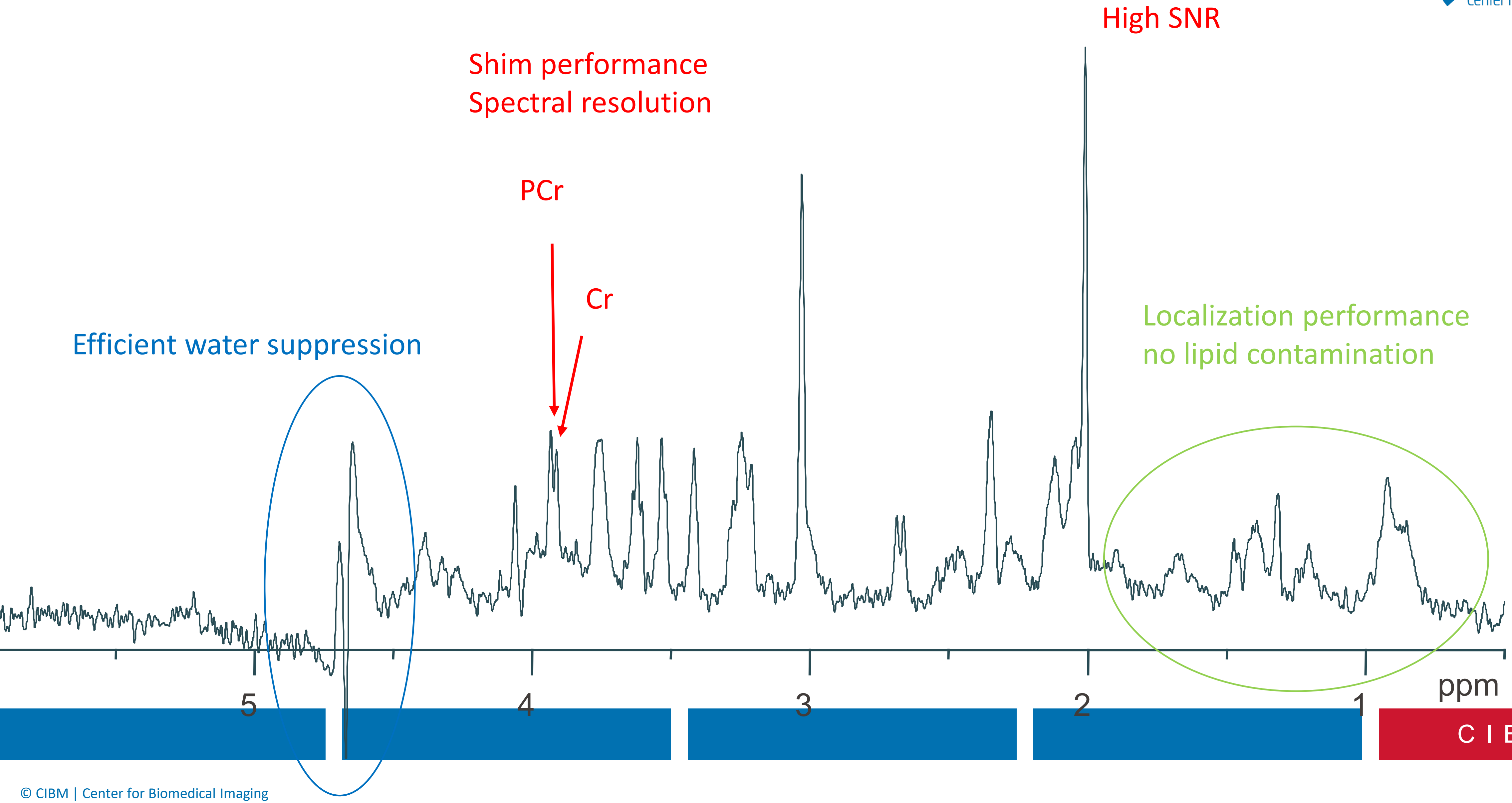

CIBM
Center for Biomedical Imaging

THANK YOU FOR YOUR ATTENTION

CHUV
UNIL | Université de Lausanne
EPFL
UNIVERSITÉ DE GENÈVE
HUG Hôpitaux Universitaires Genève

CIBM.CH